ESC European Society of Cardiology

Cardiovascular Research (2023) **119**, 2607–2622
https://doi.org/10.1093/cvr/cvad144

Cardiomyocyte and endothelial cells play distinct roles in the tumour necrosis factor (TNF)-dependent atrial responses and increased atrial fibrillation vulnerability induced by endurance exercise training in mice

Robert Lakin [1]*, Nazari Polidovitch[1], Sibao Yang[1,2], Mihir Parikh[1†], Xueyan Liu[1,2†], Ryan Debi[1], Xiaodong Gao[1], Wenliang Chen[1], Camilo Guzman[1], Simona Yakobov[1], Farzad Izaddoustdar[3], Marianne Wauchop[3], Qian Lei[4], Weimin Xu[2], Sergei A. Nedospasov[5,6], Vincent M. Christoffels[7], and Peter H. Backx [1]*

[1]Department of Biology, York University, 354 & 357 Farquharson Building, 4700 Keele Street, Toronto, ON M3J 1P3, Canada; [2]Department of Cardiology, China-Japan Union Hospital of Jilin University, Changchun, Jilin 130022, China; [3]Department of Physiology, University of Toronto, Toronto, ON M5S 3E2, Canada; [4]Department of Anesthesiology, Sichuan Academy of Medical Sciences and Sichuan Provincial People's Hospital, University of Electronic Science and Technology of China, Chengdu 610072, China; [5]Laboratory of Molecular Mechanisms of Immunity, Engelhardt Institute of Molecular Biology, Moscow 119991, Russia; [6]Division of Immunobiology and Biomedicine, Sirius University of Science and Technology, Sirius 354349, Russia; and [7]Department of Medical Biology, Amsterdam Cardiovascular Sciences, Amsterdam UMC, Amsterdam, The Netherlands

Received 11 June 2022; revised 22 June 2023; accepted 18 July 2023; online publish-ahead-of-print 15 September 2023

Time of primary review: 48 days

Aims Endurance exercise is associated with an increased risk of atrial fibrillation (AF). We previously established that adverse atrial remodelling and AF susceptibility induced by intense exercise in mice require the mechanosensitive and pro-inflammatory cytokine tumour necrosis factor (TNF). The cellular and mechanistic basis for these TNF-mediated effects is unknown.

Methods and results We studied the impact of *Tnf* excision, in either atrial cardiomyocytes or endothelial cells (using *Cre*-recombinase expression controlled by *Nppa* or *Tie2* promoters, respectively), on the cardiac responses to six weeks of intense swim exercise training. TNF ablation, in either cell type, had no impact on the changes in heart rate, autonomic tone, or left ventricular structure and function induced by exercise training. *Tnf* excision in atrial cardiomyocytes did, however, prevent atrial hypertrophy, fibrosis, and macrophage infiltration as well as conduction slowing and increased AF susceptibility arising from exercise training. In contrast, endothelial-specific excision only reduced the training-induced atrial hypertrophy. Consistent with these cell-specific effects of *Tnf* excision, inducing TNF loss from atrial cardiomyocytes prevented activation of p38MAPKinase, a strain-dependent downstream mediator of TNF signalling, without affecting the atrial stretch as assessed by atrial pressures induced by exercise. Despite TNF's established role in innate immune responses and inflammation, neither acute nor chronic exercise training caused measurable NLRP3 inflammasome activation.

Conclusions Our findings demonstrate that adverse atrial remodelling and AF vulnerability induced by intense exercise require TNF in atrial cardiomyocytes whereas the impact of endothelial-derived TNF is limited to hypertrophy modulation. The implications of the cell autonomous effects of TNF and crosstalk between cells in the atria are discussed.

* Corresponding authors. Tel: 647 244 4528, E-mail: pbackx@yorku.ca (P.H.B.); Tel: 416 526 8922, E-mail: lakinrob@yorku.ca (R.L.)
† Authors contributed equally to the manuscript.

Graphical Abstract

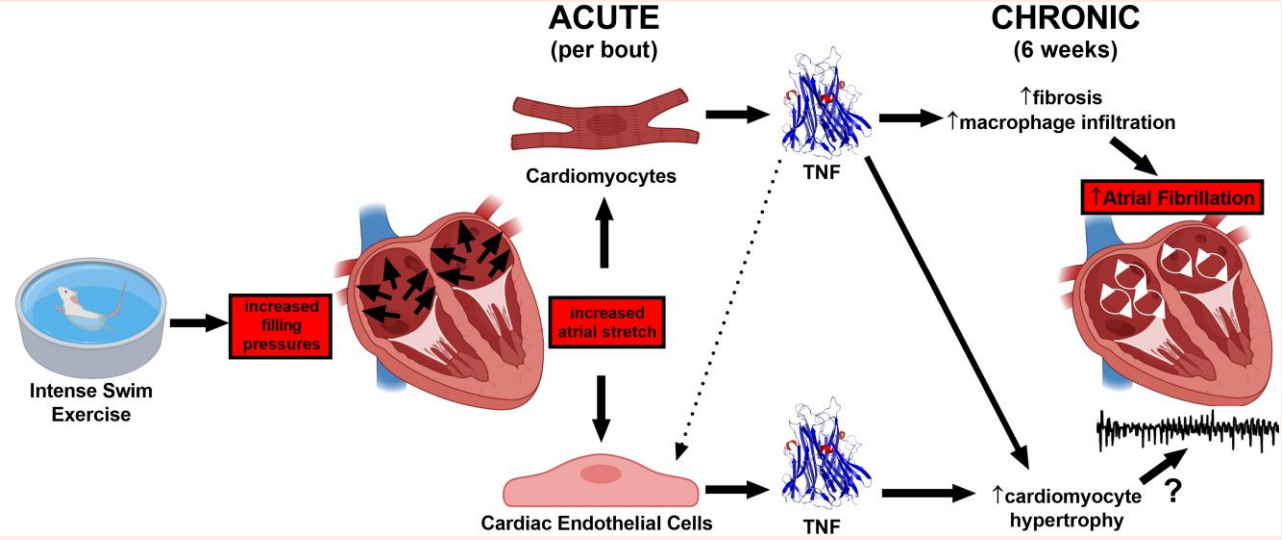

Keywords Exercise • Heart • Atrial fibrillation • Tumour necrosis factor • Inflammation

1. Introduction

Atrial fibrillation (AF) is the most frequent sustained supraventricular arrhythmia in humans, with its incidence expected to double by 2060.[1] While cardiovascular disease (CVD), poor cardiovascular health and aging are linked to an increased risk of AF,[2] it is now clear that endurance athletes paradoxically have an AF risk similar to CVD patients,[3,4] despite profoundly better ventricular function and cardiovascular health.[5] Although the mechanistic basis for an increased prevalence of AF with endurance sport is largely unknown, endurance exercise induces both atrial enlargement and elevated cardiac parasympathetic nerve activity (PNA).[6] As in humans, intense exercise in rodents also leads to physiological ventricular remodelling as well as increased cardiac PNA and atrial hypertrophy,[7] but these adaptations are accompanied by atrial fibrosis and inflammation, both hallmarks of AF in CVD patients.[8]

The relationship between AF in endurance athletes vs. CVD patients is unclear, and the underlying mechanisms remain largely unknown. Nevertheless, a common feature of most cardiovascular disease conditions linked to AF is elevated atrial pressures.[9] In this regard, intense exercise is known to cause a marked elevation in venous filling pressures (to 20–40 mmHg),[10,11] as required for enhancing cardiac output needed during exercise. Such elevations in filling pressure have been shown to cause a two-fold greater expansion of atria compared to ventricles,[7,12] which can readily explain the differential responses of atria vs. ventricles to exercise given that stretch is a powerful stimulus for hypertrophy, fibrosis, and inflammation.[13,14] Involvement of stretch in exercise-mediated atrial changes is supported by our previous studies showing that blocking tumour necrosis factor (TNF),[7,15] a well-known mechanosensitive[16] and pro-inflammatory cytokine,[7] protected against adverse remodelling and AF vulnerability induced by endurance exercise. Interestingly, numerous previous studies in animal and humans have implicated TNF in the pathogenesis AF.[17]

In this study, we focused on the cellular origins of the TNF responsible for stretch-mediated AF and atrial remodelling associated with exercise. Since both cardiomyocytes and endothelial cells[18] respond strongly to stretch, with their architectural arrangement facilitating multidirectional paracrine and mechanical crosstalk between cell types,[19] we exercised mice with *Tnf* excision in either atrial cardiomyocytes (using *NPPA-Cre*) or endothelial cells (using *Tie2-Cre*). Our results establish that excision of *Tnf* in atrial cardiomyocytes prevents atrial hypertrophy, fibrosis, and increased macrophage numbers as well as increased AF vulnerability induced by exercise training, without affecting the beneficial physiological ventricular remodelling or elevated cardiac PNA activity. In contrast, *Tnf* excision specifically in endocardial and endothelial cells only prevented exercise-induced atrial hypertrophy. These observations highlight cell autonomous and non-redundant roles of TNF in exercise-induced AF. Moreover, unlike AF in both patients and animal heart disease models,[20,21] the NLRP3 inflammasome was not activated with chronic exercise, although trends of NLRP3 inflammasome activation were observed with bouts of acute exercise in both atria and ventricles.

2. Methods

2.1 Experimental animals

This study was carried out in adherence with the current guidelines of the Canadian Council of Animal Care and NIH. The protocol was approved by the Animal Care Committee at York University (2016-3). Studies began with 6-week-old male mice (body weight = 30–35 g) in a CD1 background (back-crossed a minimum of eight times). Mice were housed at a constant temperature (22 ± 1°C) with a 12 h:12 h light–dark cycle and fed with a standard laboratory mouse diet *ad libitum* with free access to water.

2.2 Genotypes of CD1 mice and the generation of Tnf excision in atrial myocardium and endothelial cells

We used mice with floxed TNF genes ($Tnf^{flox/flox}$) generated previously.[22] Atrial-specific *Tnf* excision was achieved by generating $Tnf^{flox/flox}$ mice that heterologously express *Cre*-recombinase under the control of a truncated promoter of the *Nppa* gene (*Nppa-Cre*), driving expression in atrial (but not ventricular) cardiomyocytes.[23] Endothelial cell-specific *Tnf* excision was achieved by crossing $Tnf^{flox/flox}$ mice with *Tie2-Cre* mice [B.6 Cg-Tg (*Tek-cre*)

12Flv/J, Stock#004128, Jackson Laboratories].[24] Littermate control *Tnf*$^{flox/flox}$ mice did not express *Cre*-recombinase (i.e. *Cre*−).

Genotyping was performed by placing tail samples into 300 µL of 0.05 M NaOH and heating to 95°C for 1–1.5 h. After neutralizing the pH with 100 µL of 0.5 M Tris-HCl buffer (pH 8.0), 2 µL of supernatant was used for PCR-based detection as described previously.[16] Primers for detection of *Tnf*$^{flox/flox}$ and *Cre* are outlined in the Supplementary material online, *Supplementary Methods*.

Cre expression in atrial cardiomyocytes was confirmed using immunohistochemistry for *Cre* (1:1000, Cell Signaling Cat#15036) in paraffin embedded fixed (4% paraformaldehyde, PFA) heart tissue (5 µm) slices with secondary anti-rabbit IgG antibody (1:1000 Abcam Cat#ab150075) for detection. Tissue slices were labelled with WGA (1:500) and DAPI (Abcam Cat#ab104139) to visualize the cell membrane and nuclei, respectively. *Cre* expression was seen in the atria (but not ventricles) of mice possessing the *Nppa-Cre* transgene (*Nppa-Cre*+ mice) (see Supplementary material online, *Figure S1A*). In contrast, *Cre* expression was seen in both the atria and ventricles of mice expressing the *Tie2-Cre* transgene (*Tie2-Cre*+) (see Supplementary material online, *Figure S1A*). No evidence of *Cre* expression was detected without (*Cre*−) the *Nppa-Cre* or *Tie2-Cre* transgenes.

Tnf excision in *Nppa-Cre* mice was further assessed by performing qtPCR on genomic DNA (Invitrogen cat#K1820-01) samples isolated from tissues and cardiomyocytes after enzymatic digestion. *Tnf* expression in atrial tissue from *Nppa-Cre*+ mice was reduced by ∼50% compared to ventricles while being reduced by >70% in DNA isolated from atrial cardiomyocytes compared to ventricular cardiomyocytes (see Supplementary material online, *Figure S1B*). While these findings might suggest incomplete *Tnf* excision in atrial cardiomyocytes in *Nppa-Cre*+ mice, our estimates are expected to be affected by the presence of other cell types in tissues and incomplete cardiomyocyte purification following digestion. We previously demonstrated *Tnf* excision in endothelial cells in *Tie2-Cre*+ mice.[25] When interpreting our results, we considered the impact of possible incomplete excision.

2.3 Swim exercise protocol

Swim training was performed during the light phase of the light–dark cycle. Mice were randomized to eight experimental groups: (i) *Tnf* excision (*Nppa-Cre*+ or *Tie2-Cre*+) sedentary, (ii) *Tnf* excision (*Nppa-Cre*+ or *Tie2-Cre*+) swim training, (iii) littermate *Cre*− sedentary, and (iv) littermate *Cre*− swim training. Mice swam in containers (30 cm diameter) filled with water at 32–33°C circulating at ∼15–20 L/min generated by a central submersible water pump. We have previously shown that when mice swim against water currents (see *Supplementary* material online, *Video S1*), their stress hormone (i.e. faecal corticosterone) levels are not elevated,[26] unlike what has been reported in other forced swim protocols (i.e. tail-weights, water bubbling, and detergents). Swim training started with sessions lasting 30 min that subsequently increased by 10 min per day until the session length reached 90 min. Thereafter, the mice swam for 90 min twice daily (separated by 4 h) for the following 6 weeks on weekdays. For studies exploring the acute effects of swimming exercise, mice were familiarized for 10 min per day for 3 days, followed by 2 days of two 90 min swim sessions daily separated by 4 h. Sedentary mice were placed in swim containers without water current twice daily for 5 min.

2.4 Echocardiography

Left ventricular (LV) functional and morphological remodelling was assessed as previously described.[7] Briefly, mice were anaesthetized with 1.5% isoflurane oxygen mixture and placed on a heated stage that maintained body temperature between 36.9 and 37.3°C. Transthoracic M-mode echocardiographic examination was conducted using a 30 MHz ultrasonic linear transducer scanning head (Vevo2100, VisualSonics). All LV functional indices, chamber size, and wall diameter measurements were collected in the long-axis view and analysed using the VisualSonics cardiac analysis suite.

2.5 Invasive haemodynamic assessments

As done previously,[7] mice were anaesthetized using 1.5% isoflurane oxygen mixture and maintained between 36.9 and 37.3°C. The right common carotid was dissected and cannulated using a 1.2 F pressure catheter (Transonic) that was subsequently advanced into the LV. Data were analysed using LabScribe3 (iWorx) software.

2.6 Telemetric haemodynamics

To assess haemodynamic changes during intense exercise, radiofrequency emitting haemodynamic telemetry devices (PA-C10, Data Sciences International, DSI) were implanted sub-dermally into the interscapularis region, as previously described.[10] Briefly, mice were anaesthetized (2.5% isoflurane in oxygen), given a loading dose of Metacam (2 mg/kg sc), and maintained on a heating pad at 37°C. The fluid-filled catheter was inserted into the right common carotid artery and advanced into the LV. After recovery (7–10 days), a 30 min baseline recording preceded an acute 30 min swim session. LV end-diastolic pressure (LVEDP) was used as an index of left atrial pressure. Data were analysed using Ponemah Physiology Platform Plus (P3) analysis software (v6.4; DSI).

2.7 Electrocardiography

Surface ECG measurements were conducted on anaesthetized mice (1.5% isoflurane oxygen mixture) at a steady temperature (36.9–37.3°C) using sub-dermal platinum electrodes (NeuroSource Medical) in the lead II arrangement. Digitized data were continuously collected (Gould ACQ-7700) and analysed using Ponemah P3 software (DSI). To assess cardiac autonomic modulation of heart rate (HR), the HRs of anaesthetized mice were determined at baseline and following sequential pharmacological blockade with atropine sulfate (2mg/kg, ip) and propranolol hydrochloride (10mg/kg, ip) (Sigma-Aldrich) to inhibit parasympathetic and sympathetic cardiac regulation, respectively.

2.8 Cardiac electrical remodelling and arrhythmia vulnerability

Electrical properties and arrhythmia vulnerability were assessed as previously described.[15] Briefly, following anaesthetization (1.5% isoflurane oxygen mixture), the right jugular vein was isolated and a 2.0 F octapolar recording/stimulation EP catheter (CI'BER Mouse, Numed) was inserted and advanced into the right ventricle. Programmed electrical stimulations were delivered to either the right atria or right ventricle to assess arrhythmia vulnerability. All stimulations were delivered at a magnitude of 1.5× capture threshold and 1 ms pulse duration. Effective refractory periods (ERPs) were determined by delivering nine pulses at 20 ms below the R-R interval followed by an extra stimulation. The S2 coupling interval was initially delivered above capture (∼40 ms) and reduced by 5 ms increments until capture. For arrhythmia induction, 27 pulses at 40 ms intervals were applied to each chamber and reduced at 2 ms decrements to 20 ms. In the absence of inducibility, 20 trains (every 1.5 s) of 20 pulses (2 ms duration) at a 20 ms interpulse interval were applied. Only reproducible episodes of rapid, chaotic, and continuous atrial or ventricular activity ≥ 10 s were defined as a sustained arrhythmic event.

2.9 Optical mapping

Heparinized mice were euthanized with an anaesthetic overdose of isoflurane (∼5%). After deep anaesthesia was achieved, the thorax was opened by mid-sternal incision. The heart was quickly excised into warn (35°C) Tyrode's solution (in mmol/L): 140 NaCl, 5.4 KCl, 1.2 KH_2PO_4, 1 $MgCl_2$, 1.8 $CaCl_2$, 5.55 D-glucose, 5 HEPES, and 10 U/mL heparin (pH 7.4). The heart was pinned to a Sylgard coated Petri dish, and the pericardium and any other residual tissue were excised. The atria were separated from the ventricles by making an incision along the connective tissue in the atrioventricular groove. Atria were pinned to reveal the mitral and tricuspid valves, and atrial fat pads and residual tissue were removed. Next, the orientation of the atria was flipped to expose the pulmonary veins, the

mitral and bicuspid valves were removed, and any additional residual tissue was excised. Finally, incisions were made in a straight path along the superior and inferior vena cava to 'open' the atria. Atria were then transferred to a separate dish and superfused continuously with carbogenized (95% O_2/5% CO_2) Krebs solution at 35°C (in mmol/L): 118 NaCl, 4.2 KCl, 1.2 KH_2PO_4, 1.5 $CaCl_2$, 1.2 $MgSO_4$, 2.3 $NaHCO_3$, 20 D-glucose, and 2 Na-pyruvate (pH 7.35–7.4).

For optical mapping experiments, isolated atrial were stained for 10 min with voltage-sensitive dye (10 μM, Di-4-ANEPPS, Sigma-Aldrich) and then continuously superfused at a constant volume and flow rate with carbogenized Krebs solution (35°C, pH: 7.35–7.4). Atria were paced at 90 ms intervals from the left atrial appendage, and images were captured using a high speed camera (1000 frames/s) (MiCAM Ultima-L, SciMedia) in order to generate activation maps and calculate conduction velocities. Atria arrhythmia inducibility was assessed and characterized as described above. Images were acquired using the Ultima Acquisition system (Brainvision), and data were analysed using BV_Analyze (Brainvision, Tokyo, Japan) or Rhythm (Washington, DC, USA) software.

2.10 Morphometry and histological assessments

After functional assessments were completed, animals were weighed and euthanized with an anaesthetic overdose of isoflurane (~5%). After deep anaesthesia was achieved, the thorax was opened via a complete bilateral thoracotomy, the inferior vena cava cut, and 1% KCl in 0.01 M PBS was administered transapically. Hearts were excised, blotted dry, and weighed, and the atria and ventricular tissue were separated to weigh individual chambers. The right tibia was harvested and measured for heart weight normalization (*Table 1*).

For histology, hearts were perfused with PBS containing 1% KCl followed by 4% PFA in 0.01 M PBS and stored overnight in 4% PFA in 0.01 M PBS at 4°C. Hearts were then embedded in paraffin, and 5 μm thin sections were stained with Picrosirius red (PSR) for collagen visualization and quantification. The atria were imaged using an Aperio AT2 brightfield whole slide scanner (Leica Biosystems) (20×; 0.5 μm/pixel) and analysed with Aperio ImageScope. Collagen expression was quantified using ImageJ software as the ratio of positively stained tissue area to total tissue area of each section using the threshold method.[7]

To visualize macrophage infiltration, F4/80$^+$ staining was used. A Nikon A1R (Nikon) confocal laser scanning microscopy system was used to acquire the whole atrium image of each section by combining both XY stitching and Z stack function. To quantify macrophage infiltration, F4/80$^+$ cell counts per mm^2 of tissue area were determined for each slice. For ventricular assessments, 5–10 images were randomly sampled from the LV of each section and quantified as above.

2.11 p38MAPK western blot analysis

Atrial samples were isolated and snap frozen in liquid nitrogen. Protein was extracted in a cell lysis buffer (20 mM Tris-HCl, pH 7.5, 150 mM NaCl, 1 mM Na_2EDTA, 1 mM EGTA, 1% Triton, 50 mM NaF, 1 mM Na_3VO_4, 1 mM PMSF, 2 mM benzamidine, 1 μg/mL leupeptin) and centrifuged at 12 000×*g* for 15 min. Next, supernatants were extracted, and protein concentration was measured using Bio Rad ABS Protein Assay reagent (#5000114, #5000113, #5000115). Each sample (40 μg) was resolved by 10% sodium dodecyl sulfate-PAGE (SDS-PAGE) and transferred to nitrocellulose membranes that were incubated with the following primary antibodies: phosphorylated p38MAPK (1:1000, BD #612281), endogenous p38MAPK (1:1000, #9212, Cell Signaling Technology, USA) and with secondary antibodies anti-mouse or anti-rabbit (1:10 000, #926-32210, #926-68071, Mandel Scientific). The membrane was scanned on a LICOR Odyssey Infrared Imaging System, with different fluorescent channels (700 and 800 nm) used to visualize total p38 and phospho-p38 on the same blot. Band analysis was performed using Image Studio Lite software (v5.2).

2.12 NLRP3 inflammasome western blot analysis

Atria and ventricles were isolated from sedentary and 6-week swim-trained mice and frozen in liquid nitrogen. Tissues were homogenized using Pierce™ RIPA buffer (89900, Thermo Scientific) supplemented with protease inhibitor and PMSF. After centrifugation at 12 000 rpm for 20 min at 4°C, supernatants were extracted, and protein concentrations were determined using DC protein assay kit (5000111, Bio Rad). A total of 40 μg/well of atrial and ventricular tissue lysates were subjected to electrophoresis on 12.5% SDS-PAGE and transferred onto PVDF membranes. Blots were incubated with primary antibodies against the following proteins: NLRP3 (1:2000, CST #15101, Cell Signaling Technology), IL-1β (1:1000, #31202S, Cell Signaling Technology), and Caspase-1 (1:1000, #sc-56036, Santa Cruz Biotechnology). GAPDH was detected using ab Anti-GAPDH antibody (1:1000, #ab8245, abcam). Immobilon Forte Western HRP substrate and SuperSignal West Pico PLUS chemiluminescent substrate were used for detection, and band analysis was performed using ImageLab 6.1, Bio Rad.

2.13 RNA sequencing of NLRP3 inflammasome

Tissue harvesting, RNA extraction, RNA library preparation and sequencing, and analysis of RNA-sequencing data in 2-day (four-session) and 2-week mice were undertaken, as previously described[27] (see Supplementary material online, *Supplementary Methods*).

2.14 Quantitative real-time PCR

Total RNA was isolated from the atria and ventricles of Cre− and *Nppa*-Cre+ sedentary and acute (2-day, four-session) swim mice using the RNeasy Mini Kit (#74104, Qiagen) according to the manufacturer's instruction, and cDNAs were generated using High-Capacity cDNA Reverse transcription kit (Applied Biosystems, #4368814). qPCR was conducted in triplicated in 384-well plates using CFX384™ Real-Time System, Bio-Rad Laboratories. Relative mRNA transcript levels (normalized to GAPDH) were determined with quantitative real-time PCR using PowerUp SYBR Green Master Mix (Applied Biosystems, #A25741). The expression levels were measured using the ΔΔCT method, and data were reported as fold change. Primer sequences can be found in Supplementary material online, *Supplementary Methods*.

2.15 Serum tumour necrosis factor (TNF) levels

Blood samples were collected from abdominal vena cava of Cre− and *Nppa-Cre*+ sedentary and acute (2-day, four-session) swim mice at 24 h post-exercise in EDTA coated tubes (#16.444.100, Sarstedt). Plasma was centrifuged for 15 min at 3300 rpm, and samples were stored at −80°C until further analyses. TNF was measured using ELISA Kit (MTA00B, R&D Systems) according to manufacturer's instructions. The standard series were made according to the manufacturer's instructions. Briefly, the lyophilized TNF was reconstituted with $ddHdH_2O$ to a stock solution of 7000 pg/mL. Calibrator diluent RD6-12 was used to produce a dilution series with the following concentrations: 700, 350, 175, 87.5, 43.8, 21.9, and 10.9 pg/mL.

2.16 Tissue tumour necrosis factor (TNF) levels

Atrial and ventricular tissue homogenates of Cre− and *Nppa*-Cre+ sedentary and acute (2-day, four-session) swim mice were prepared in RIPA buffer with protease inhibitor using a polytron homogenizer to extract both soluble and membrane forms of TNF protein. Lysate samples were sonicated for two rounds of 10 s at 20% amplitude. Samples were subjected to ELISA for quantification of tissue TNF (MTA00B, R&D Systems) according to the manufacturer's instructions. The standard series were made

Table 1 Effects of swim exercise on left ventricular structure and function

	Cre– (NPPA controls)		*Nppa-Cre*+		*Cre*– (*Tie2* controls)		*Tie2-Cre*+	
	Sedentary	**Swim**	**Sedentary**	**Swim**	**Sedentary**	**Swim**	**Sedentary**	**Swim**
Body parameters *n*	8	8	8	8	4	6	4	6
Body weight (BW) (g)	39.7 ± 0.6	34.6 ± 0.3*	38.6 ± 0.8	34.0 ± 0.5**	38.9 ± 0.9	35.1 ± 0.4*	39.1 ± 0.7	34.6 ± 0.4
Tibia length (mm)	19.2 ± 0.1	19.3 ± 0.1	19.3 ± 0.1	19.2 ± 0.1	19.1 ± 0.1	19.2 ± 0.1	19.2 ± 0.1	19.2 ± 0.1
Ventricle weight (mg)	164.2 ± 3.4	149.9 ± 3.7*	160.2 ± 3.6	155.3 ± 3.8	161.2 ± 3.6	148.3 ± 3.5*	165.1 ± 3.9	153.6 ± 3.8
Ventricle/tibia length (mg/mm)	8.55 ± 0.26	7.77 ± 0.27	8.30 ± 0.23	8.09 ± 0.24	8.44 ± 0.29	7.72 ± 0.30	8.60 ± 0.32	8.00 ± 0.29
Echocardiography *n*	12	17	15	17	14	18	14	24
LVDd (mm)	4.26 ± 0.05	4.50 ± 0.06*	4.24 ± 0.06	4.41 ± 0.04**	4.16 ± 0.09	4.48 ± 0.07	4.13 ± 0.07	4.48 ± 0.08
LVDs (mm)	2.83 ± 0.09	3.10 ± 0.07*	2.83 ± 0.08	2.99 ± 0.04	2.68 ± 0.09	3.03 ± 0.07	2.68 ± 0.07	3.07 ± 0.07
EF (%)	62.8 ± 1.9	59.2 ± 1.2	62.3 ± 1.7	60.2 ± 0.7	65.4 ± 1.2	61.0 ± 0.9	64.9 ± 1.5	59.7 ± 0.9
FS (%)	33.8 ± 1.4	31.3 ± 0.8	33.5 ± 1.2	32.1 ± 0.4	35.6 ± 0.9	32.7 ± 0.6	35.2 ± 1.1	31.8 ± 0.6
CO (mL/min)	26.5 ± 1.0	25.7 ± 0.7	26.2 ± 0.7	25.0 ± 0.7	27.0 ± 1.2	24.4 ± 1.3	25.6 ± 0.9	22.6 ± 1.3
HR (BPM)	537 ± 19	475 ± 16*	529 ± 17	471 ± 11**	539 ± 16	434 ± 13	522 ± 17	414 ± 18
LVPWth (mm)	0.82 ± 0.02	0.77 ± 0.03*	0.81 ± 0.02	0.77 ± 0.01**	0.80 ± 0.01	0.77 ± 0.02	0.80 ± 0.01	0.76 ± 0.01
Haemodynamics *n*	9	12	11	19	9	7	7	9
MAP (mmHg)	93.6 ± 3.2	102.1 ± 3.2	95.9 ± 3.2	92.1 ± 3.6	92.0 ± 4.1	91.5 ± 4.3	92.4 ± 3.6	94.1 ± 3.1
LVPs (mmHg)	113.2 ± 2.3	114.8 ± 3.4	109.3 ± 2.9	108.0 ± 2.6	106.4 ± 3.0	104.9 ± 4.2	105.8 ± 3.2	108.1 ± 2.6
LV +dP/dt$_{max}$ (mmHg/s)	8930 ± 374	10 166 ± 316*	9073 ± 296	10 077 ± 256**	9047 ± 470	10 295 ± 413	9834 ± 371	10 310 ± 573
LV −dP/dt$_{min}$ (mmHg/s)	−9638 ± 463	−12 147 ± 508*	−9670 ± 262	−1088 ± 385**	−9285 ± 545	−9625 ± 625	10 151 ± 582	11 199 ± 821
Dob +dP/dt$_{max}$ (mmHg/s)	13 980 ± 673***	14 623 ± 492***	14 824 ± 611***	14 987 ± 282***	12 758 ± 557***	13 007 ± 305***	13 242 ± 796***	13 905 ± 858***

CO, cardiac output; EF, ejection fraction; FS, fractional shortening; HR, heart rate; LVDd, left ventricular end-diastolic diameter; LVDs, left ventricular end-systolic diameter; LVPWth, left ventricular posterior wall thickness; LVPs, left ventricular systolic pressure; LV +dP/dt$_{max}$, maximum rate of left ventricular pressure development; LV −dP/dt$_{min}$, minimum rate of left ventricular pressure development; MAP, mean arterial pressure.

*$P < 0.05$ Student's *t*-test vs. *Cre*– for *Nppa* or *Tie2* sedentary.

**$P < 0.05$ Student's *t*-test vs. *Nppa-Cre*+ or *Tie2-Cre*+ sedentary.

***$P < 0.05$ two-way ANOVA pre–post dobutamine.

according to the manufacturer's instructions. Briefly, the lyophilized TNF was reconstituted with ddHdH_2O to a stock solution of 7000 pg/mL. Calibrator diluent RD5K was used to produce a dilution series with the following concentrations: 700, 350, 175, 87.5, 43.8, 21.9, 10.9, and 5.45 pg/mL.

2.17 Statistics

Data are presented as mean ± S.E.M. Continuous variables were compared between multiple groups of mice (i.e. sedentary and swim-trained *Nppa-Cre+* and *Cre−* or *Tie2-Cre+* and *Cre−*) with a two-way analysis of variance (ANOVA), and subsequent pairwise comparisons were adjusted with the Sidak's multiple comparison approach. Homogeneity of variance was assessed using Levene's test. AF durations were assessed using a Mann–Whitney *U* test with Dunn's multiple comparison test as the data were not normally distributed (D'Agostino and Pearson omnibus normality test). To compare arrhythmic events, a 2 × 2 contingency table with Fisher's exact test was used. A repeated measures one-way ANOVA with Sidak's multiple comparison test was used to analyse changes in pressure and heart rate in telemetry-implanted mice. A Wilcoxon signed-rank test was used to compare pre–post changes in arrhythmia durations following atropine administration. *P* values < 0.05 were considered statistically significant. All statistical analyses were carried out using GraphPad Prism (GraphPad Software, Inc.).

3. Results

3.1 Tnf ablation in atrial cardiomyocytes attenuates exercised-induced atrial changes without affecting physiological remodelling of ventricles

Consistent with previous studies,[26,28] exercise training caused reductions ($P = 0.002$) in HR (see Supplementary material online, *Figure S2A*) in wild-type control mice (i.e. flox/flox *Cre−*). These HR changes were linked to elevated ($P = 0.049$) PNA and reductions ($P = 0.034$) in sympathetic nerve activity (SNA) (see Supplementary material online, *Figure S2B*). Importantly, compared to *Cre−* littermates, mice with *Tnf* excision in atrial cardiomyocytes (i.e. flox/flox *NPPA-Cre+*) showed the same alterations in HR ($P = 0.237$) as well as control of HR by the cardiac autonomic nervous activity ($P = 0.477$) following exercise training as the Cre- mice (see Supplementary material online, *Figure S2*). Moreover, beating rates of isolated (denervated) atria showed no differences ($P = 0.851$) between *Cre−* and *Nppa-Cre+* with or without exercise (see Supplementary material online, *Figure S2C*), establishing that exercise-induced changes in autonomic nervous HR regulation occur independently of TNF originating from atrial cardiomyocytes. The slight dilation and small changes in ejection fractions seen with exercise training (i.e. 'athlete's heart' phenotype[5]) were also similar ($P \geq 0.472$) between *Nppa-Cre+* and *Cre−* mice, as were enhancements in LV contractility (dP/dt_{max}) and relaxation (dP/dt_{min}), with and without dobutamine infusion (*Table 1*). These findings establish that atrial cardiomyocyte-specific *Tnf* excision does not affect exercise-induced physiological remodelling of the LV.

Figure 1A shows representative intracardiac bipolar electrograms following programmed electrical stimulations to assess the inducibility of AF, which was identified by rapid irregular electrical activity lasting for at least 10 s. Exercise increased ($P = 0.028$) AF inducibility in *Cre−* mice (7/15 in exercised vs. 0/15 in sedentary), and this effect of exercise was abolished ($P = 0.013$) completely in *Nppa-Cre+* mice (0/17 in exercised) (*Figure 1B* and *C*). In contrast, ventricular arrhythmias could not be evoked in either *Nppa-Cre+* or *Cre−* mice, with or without exercise (see Supplementary material online, *Figure S3*).

To understand the basis for the protection against AF inducibility in *Nppa-Cre+* mice, we assessed tissue properties. As expected from previous studies,[7] *Figure 2* shows that exercise-trained wild-type (*Cre−*) mice had increased ($P < 0.028$) atrial weights (normalized to tibia lengths) as well as increased atrial to ventricular weights ratios (*Figure 2A* and *B*), mirroring the hypertrophy seen in human endurance athletes.[5] This difference in exercise-induced hypertrophy between atria and ventricles was associated with elevated ($P = 0.0003$) fibrosis (*Figure 2D*) as well as enhanced ($P = 0.009$) macrophage infiltration ($F4/80^+$ cells) (*Figure 2E*) in atria, neither of which was observed in exercised ventricles. Consistent with the protection against atrial arrhythmia inducibility, *Tnf* ablation in atrial cardiomyocytes abolished ($P < 0.05$) atrial hypertrophy (both atrial weights and atrial/ventricular weight ratios), prevented ($P = 0.0009$) atrial fibrosis, and decreased ($P = 0.023$) macrophage infiltration in exercise-trained mice (*Figure 2*). As might be expected, no differences in fibrosis or inflammatory cell numbers were observed in LVs between exercise trained and sedentary mice in either the *Nppa-Cre+* or *Cre−* mice, although a trend ($P > 0.131$) for increased macrophage counts was seen with exercise in both groups (see Supplementary material online, *Figure S4*). Nonetheless, atria showed a three-fold greater increase in infiltrating macrophages compared to the LV with exercise, establishing clear differences in inflammatory cell responses to exercise between the chambers. See Discussion.

To characterize the induced AF events seen in exercised mice in greater detail, we investigated the electrical properties of isolated atria. Consistent with the *in vivo* assessments, field recordings of isolated atria revealed that sustained atrial arrhythmias could be readily induced ($P = 0.026$) in atria isolated from exercised (4/7) *Cre−* but not sedentary (0/8) *Cre−* mice (*Figure 3A* and *B*). Optical mapping revealed that these arrhythmias were characterized by complex and dynamic electrical activity involving rapid focal activity, re-entry, rotors, and conduction block (*Figure 3C*), not unlike the patterns reported in other animal models of AF.[29] More important, atria from exercise-trained *Cre−* mice had slower ($P < 0.0001$) conduction velocities (CVs) compared to sedentary *Cre−* atria (*Figure 3D* and *E*), as might be expected from the increased fibrosis. Exercised *Cre−* atria also displayed prolonged action potential durations (APDs), measured at 90% repolarization (APD_{90}), compared to sedentary *Cre−* mice (*Figure 3F*), which could also contribute to conduction slowing and block. Also congruent with the *in vivo* measurements and the fibrosis results, atrial arrhythmias could not be induced in atria isolated from either exercised (0/6) or sedentary (0/6) *Nppa-Cre+* mice and this coincided with the comparable CVs ($P = 0.106$) between exercised and non-exercised atria from *Nppa-Cre+* mice. Nevertheless, APD_{90} was prolonged ($P < 0.01$) in exercised vs. non-exercised *Nppa-Cre+* atria (*Figure 3F*), demonstrating that APD prolongation alone is insufficient to slow conduction or enhance AF vulnerability. Also, the CVs in both groups of *Nppa-Cre+* atria had faster CVs than the exercised *Cre−* atria but not the non-exercised *Cre−* atria (*Figure 3E*).

The results in isolated atria support the conclusion that alterations in intrinsic refractoriness properties play a minimal role in promoting AF with exercise. However, enhanced cardiac PNA has been shown to promote AF[6] that is particularly relevant in AF linked to endurance sport.[4] Nonetheless, no differences ($P = 0.825$) in the atrial effective refractory periods (AERPs) were observed between the four groups of mice (see Supplementary material online, *Figure S5A*). However, following cardiac PNA blockade AERPs showed greater prolongation in swim-trained vs. sedentary mice (see Supplementary material online, *Figure S5B*) for both the *Nppa-Cre+* and *Cre−* mice and this led to reduced ($P = 0.009$) AF durations (18.9 ± 2.1 s vs. 13.6 ± 0.8 s) in the exercised *Cre−* mice (see Supplementary material online, *Figure S5C*) without affecting the percentage of mice developing AF in response to overdrive atrial pacing. These observations demonstrate that AERP can in principle impact on AF vulnerability, as expected.[30]

3.2 Endothelial-specific Tnf ablation and structural and autonomic remodelling in exercised mice

Our findings establish that TNF originating from atrial cardiomyocytes is required for adverse atrial remodelling and arrhythmia inducibility arising from exercise training. Nevertheless, it is conceivable that TNF from other

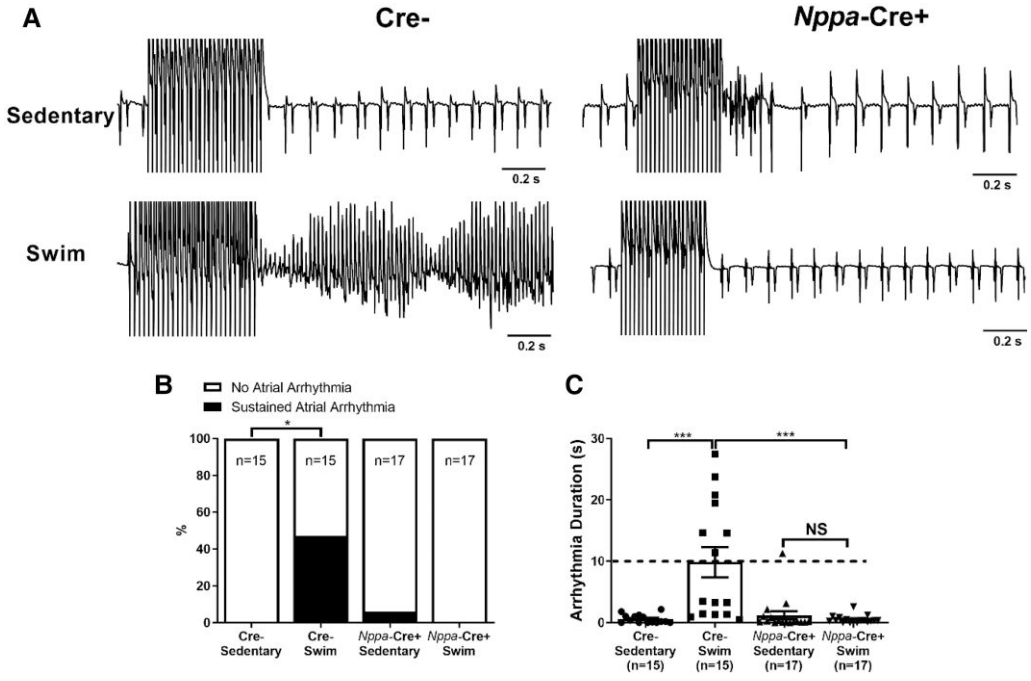

Figure 1 Atrial-specific gene ablation of *Tnf* reduces atrial arrhythmias inducibility in swim-trained mice. Atrial arrhythmia inducibility was determined using intracardiac octopolar catheters inserted into the right atria via the superior jugular vein. (*A*) Representative electrical recordings using intracardiac catheters during and following programmed electrical stimulations in sedentary and swim-exercised mice with (*Nppa-Cre+*) ($n = 17$ per group) and without (*Cre−*) ($n = 15$ per group) atrial-specific *Tnf* ablation. Prolonged highly disorganized electrical patterns lasting greater than 10 s, indicative of atrial arrhythmias, were only seen typically in swim-exercised *Cre−* mice. (*B* and *C*) Atrial-specific *Tnf* ablation prevented (*P* value from 2 × 2 contingency table using Fisher's exact test) the incidence of atrial arrhythmias lasting >10 s and decreased the duration of arrhythmia episodes. Data presented as mean ± S.E.M. *P* values for arrhythmia durations from Mann–Whitney *U* test with Dunn's multiple comparisons test. *$P < 0.05$; **$P < 0.01$.

cell types in the atria might also play a role in atrial responses to exercise training. Since we previously showed that cardiac hypertrophy in mice with Noonan syndrome mutations involves TNF-dependent interactions between endothelial cells and cardiomyocytes,[25] we studied mice with *Tnf* excision in endothelial cells. As seen with *Tnf* excision in atrial cardiomyocytes, swim-trained *Tie2-Cre+* mice had lower HRs ($P = 0.0002$) compared to sedentary controls that were linked to elevations ($P = 0.025$) in cardiac PNA and reductions ($P = 0.042$) in cardiac SNA (see Supplementary material online, *Figure S6*). Consistent with cardiac PNA involvement in the reduced HRs induced by exercise training, no differences ($P = 0.688$) were observed either in HRs between exercise-trained vs. untrained *Tie2-Cre+* mice following complete ANS blockade (see Supplementary material online, *Figure S6A*) or in beating rates ($P = 0.975$) of denervated isolated atria (see Supplementary material online, *Figure S6C*) isolated from exercised vs. non-exercise *Tie2-Cre+* mice. In addition, we observed the expected LV physiological changes, as assessed by echocardiography and invasive haemodynamics, in both *Tie2-Cre+* and *Cre−* swim mice (*Table 1*).

Exercise training of mice with endothelial-specific *Tnf* excision showed increased ($P = 0.033$) AF vulnerability, as summarized in *Figure 4* (AF induced in 7/24 exercised vs. 0/14 non-exercised *Tie2-Cre+* mice), which was associated with corresponding increases ($P = 0.002$) in atrial fibrosis (*Figure 5C* and *D*) and ($P < 0.016$) inflammatory infiltrates (*Figure 5C* and *E*). On the other hand, atria isolated from exercise-trained mice with endothelial-specific *Tnf* excision showed no evidence ($P = 0.219$) of atrial hypertrophy (*Figure 5A* and *B*) compared to sedentary controls with endothelial TNF ablation. These observations suggest that cardiac fibrosis plays a more dominant role than hypertrophy in the increased AF vulnerability associated with intense exercise training. Not unexpectedly, no differences in arrhythmia vulnerability (see Supplementary material online, *Figure S7*), fibrosis, nor macrophage infiltration were observed in the LV between these groups (see Supplementary material online, *Figure S8*).

The lack of protection afforded by endothelial-specific *Tnf* ablation to AF inducibility in mice was also seen in isolated atria. Atrial arrhythmia inducibility was higher ($P = 0.035$) in atria isolated from exercise-trained *Tie2-Cre+* (4/7) mice (*Figure 6B*) compared to sedentary *Tie2-Cre+* littermates (0/8). Isochronal activation maps (*Figure 6D*) of AF events in atria from exercised *Tie2-Cre+* mice showed conduction velocity slowing ($P < 0.003$) without differences ($P = 0.650$) in APD_{90s} compared to sedentary controls (*Figure 6E*). Similar differences were observed between exercised and non-exercised *Cre−* mice. Moreover, no differences ($P = 0.437$) in AERPS were observed between the four groups of mice (see Supplementary material online, *Figure S9A*). Nevertheless, the extent of AERP prolongation following PNA blockade was greater ($P < 0.012$) in swim vs. sedentary mice in both *Tie2-Cre+* and *Cre−* mice (see Supplementary material online, *Figure S9B*) and was associated with reduced ($P < 0.032$) durations of the AF events induced in both *Cre−* (27.2 s vs. 15.5 s) and *Tie2-Cre+* (21.6 s vs. 14.5 s) swim-exercised mice, without affecting the percentage of mice developing inducible AF (see Supplementary material online, *Figure S9C*). These results support the conclusion that AP duration influences AF sustainability once initiated, consistent with the effects of cardiac refractoriness on arrhythmia susceptibility.[30]

3.3 Exercise increases atrial pressures and causes TNF-mediated activation of p38 in atrial cardiomyocytes

The results described above establish that exercise differentially affects atria vs. ventricles in a manner that requires atrial myocyte-derived TNF. While the basis for the chamber-specific actions of exercise training is

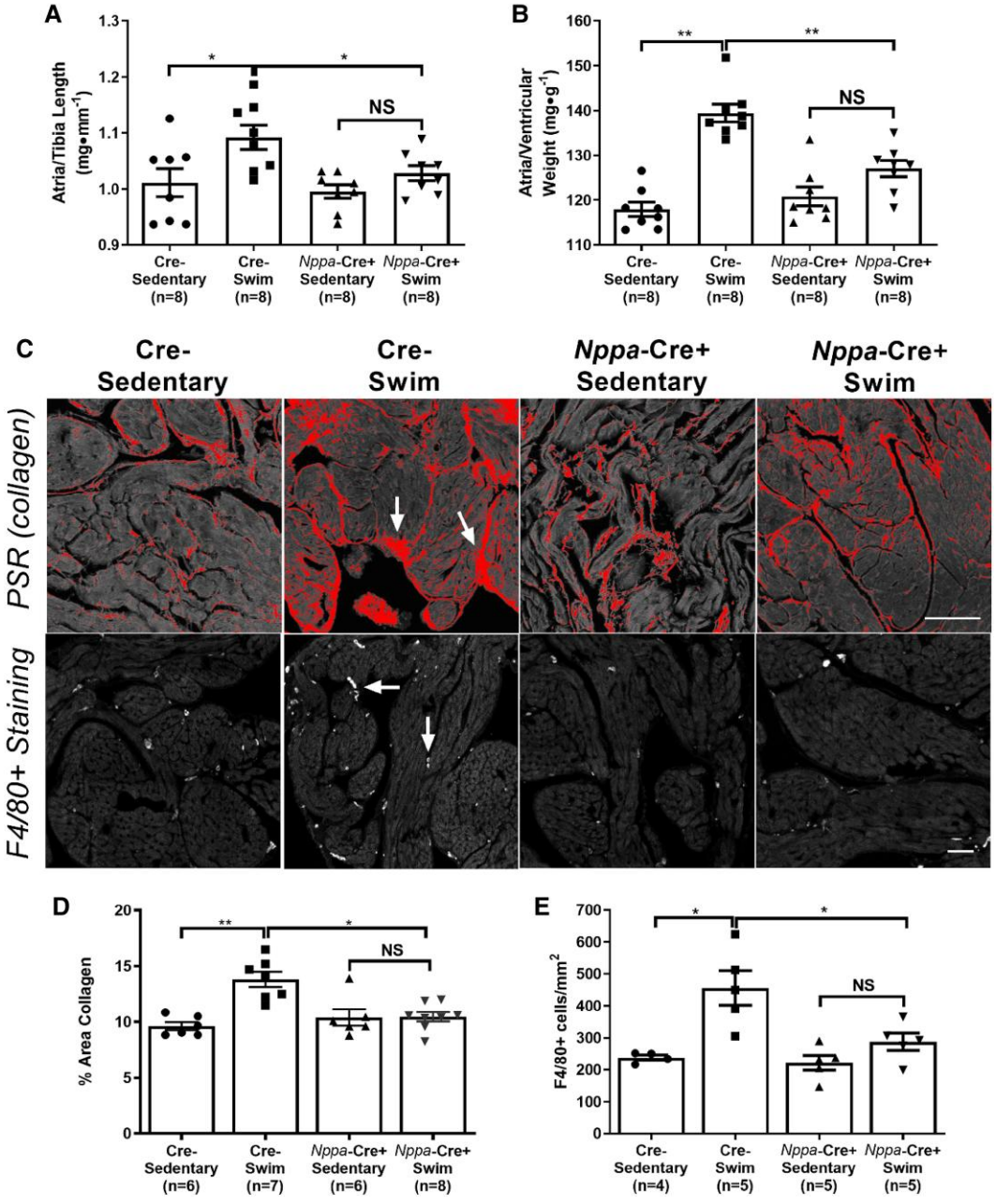

Figure 2 Atrial-specific *Tnf* gene ablation reduces exercise-induced increases in atrial hypertrophy, fibrosis, and inflammatory cell infiltration. (*A* and *B*) Atrial weights-to-tibial length and atrial weights-to-ventricular weights were increased in swim-trained vs. sedentary control (*Cre*−) mice ($n = 8$ per group). The degree of atrial hypertrophy with exercise was reduced in *Nppa-Cre*+ mice ($n = 8$ per group). (*C*) Top panel: Typical confocal micrographs of atrial sections stained with Picrosirius red (PSR). Collagen deposition (arrows) was reduced in swim-trained *Nppa-Cre*+ mice compared to swim-trained *Cre*− mice. Bottom panel: Confocal micrographs of atrial sections stained with F4/80$^+$ to quantify macrophage infiltration (arrows). Macrophage counts were reduced in *Nppa-Cre*+ compared to *Cre*− swim-trained mice. (*D*) Quantification of collagen deposition (%) shows elevations in atrial fibrosis in *Nppa-Cre*+ swim ($n = 7$) compared to *Cre*− sedentary mice ($n = 6$). However, *Tnf* ablation in atrial myocardium reduces exercise-induced elevations in atrial fibrosis, with no differences observed between *Nppa-Cre*+ swim ($n = 8$) and *Cre*− sedentary ($n = 6$) mice. (*E*) *Nppa-Cre*+ swim-trained mice ($n = 5$) showed reduced exercise-induced macrophage infiltration (F4/80$^+$ cell count) compared to *Cre*− swim mice ($n = 5$). Data presented as mean ± S.E.M. *P* values from two-way ANOVA with Sidak's multiple comparison tests. *$P < 0.05$; **$P < 0.01$; ***$P < 0.001$ as indicated. NS, not significant. Scale bar = 50 μm.

unclear, it is not unreasonable to suggest that these differential effects of exercise arise from distinct responses of atria vs. ventricles to elevations in venous filling pressures associated with exercise.[10,11] This possibility is supported by the observations that atria are far more compliant than ventricles[7,12] and that TNF is a mechanosensitive cytokine that promotes fibrosis, hypertrophy, and inflammation. To determine whether *Tnf* excision affects the haemodynamic adjustments to exercise, we measured ventricular pressures using telemetry during swimming. *Figure 7A* shows that the onset of swim exercise in *Cre*− mice causes profound and sustained elevations ($P = 0.024$) in LVEDP, an index of atrial filling pressures, and

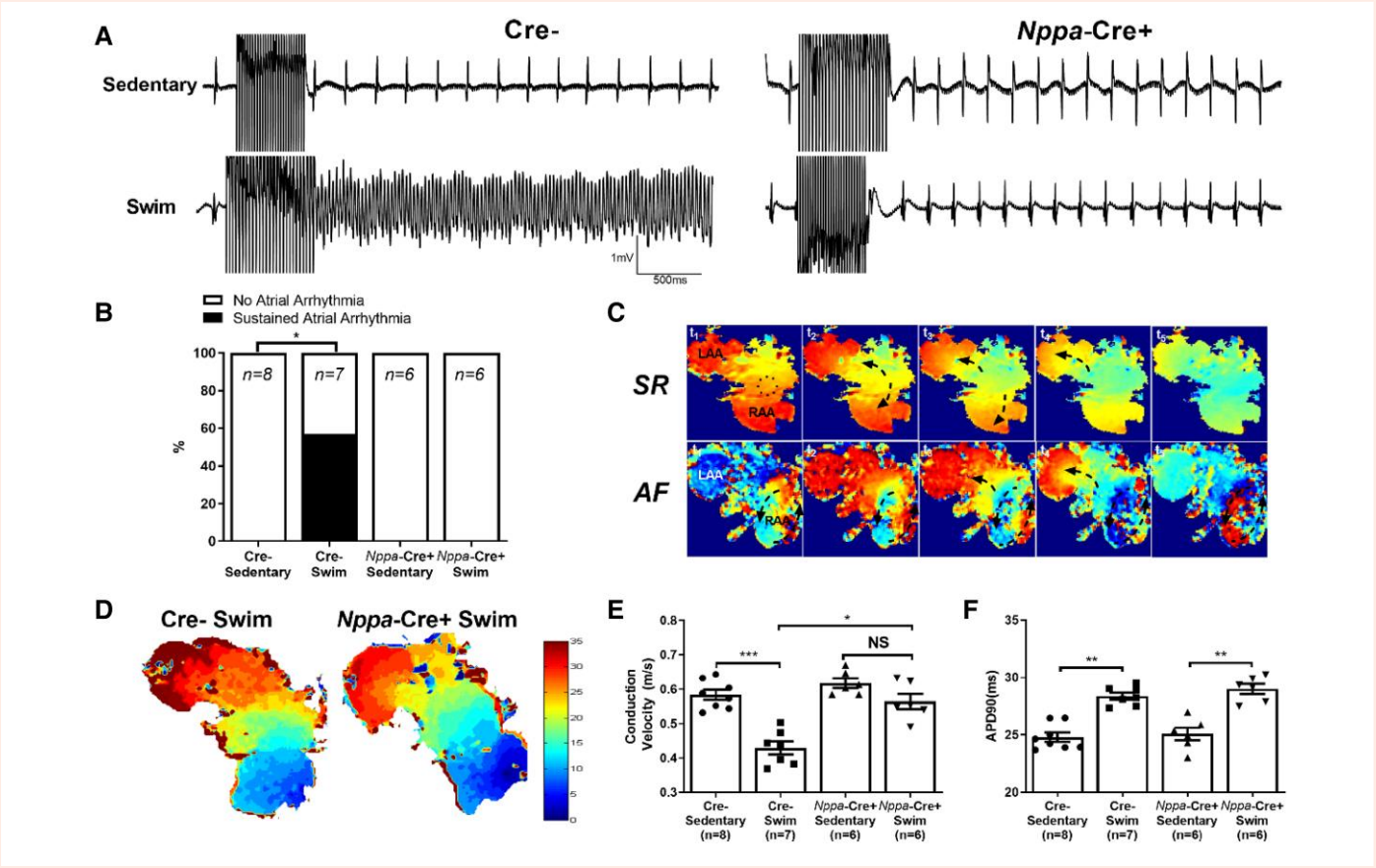

Figure 3 Effects of atrial cardiomyocyte-specific *Tnf* ablation on electrical properties on exercise-induced arrhythmias and electrical changes in isolated atria. (*A*) Representative field electrogram recordings from isolated (denervated) atria in *Nppa-Cre+* and *Cre−* sedentary and exercised mice showing atrial arrhythmia inducibility. Note evidence of sustained AF episodes in *Cre−* exercised mice only. (*B*) Atrial-specific *Tnf* ablation (*Nppa-Cre+*) reduced the sustained (>10 s) atrial arrhythmia inducibility (*P* value from 2 × 2 contingency table using Fisher's exact test) in exercised mice (*n*-values indicated in figure panel). (*C*) Representative optically-mapped images of AF episodes from rapidly stimulated isolated atria during sinus rhythm (SR) (top panel) and during AF (bottom panel). (*D* and *E*) Typical isochrone activation maps and summary results of conduction velocity (CV) measured in right atrial appendages isolated from *Nppa-Cre+* ($n = 6$) and *Cre−* ($n = 7$) swim-exercised mice revealed that CVs are slowed in *Cre−*, but not *Nppa-Cre+* swim mice when compared to their sedentary counterparts ($n = 8$ and 6 per group, respectively). (*F*) In isolated atrial preparations, action potential duration at 90% of repolarization (APD_{90}) was prolonged in exercised compared to sedentary mice, in both *Nppa-Cre+* and *Cre−* groups. The *n* value for individual groups is indicated on bar graphs. Data presented as mean ± S.E.M. *P* values from two-way ANOVA with Sidak's multiple comparison tests. $^*P < 0.05$; $^{**}P < 0.01$; $^{***}P < 0.001$.

Tnf excision in atrial cardiomyocytes did not affect haemodynamic responses to exercise. Nevertheless, when mice with *Tnf* excision in atrial cardiomyocytes are exercised, no changes ($P = 0.188$) were observed in the level of p38MAPK phosphorylation, a well-known downstream TNF-dependent factor that is activated by myocardial stretch,[31] whereas p38MAPK phosphorylation levels were increased in littermate *Cre−* mice by exercise (*Figure 7*B and Supplementary material online, *Figure S10*). On the other hand, phosphorylation levels of p38MAPK were increased ($P = 0.043$) with exercise in mice with endothelial cell-specific *Tnf* ablation as well as littermate control *Cre−* mice (*Figure 7*B and Supplementary material online, *Figure S10*). These findings suggest that the atrial-selective remodelling induced by exercise involves cell autonomous TNF-dependent signalling cascades activated by stretch.

3.4 Acute and chronic exercise does not enhance NLRP3 inflammasome signalling in mice

Our results establish a clear role for cardiomyocyte-derived TNF in exercise-induced atrial changes. Though recent studies have concluded that AF is associated with the NLRP3 inflammasome[20,21] that overlaps with TNF-dependent signalling,[32] we found that the atrial levels of NLRP3 procaspase-1 and IL-1β were unaffected ($P > 0.258$) by exercise (see Supplementary material online, *Figure S11*). As expected from the absence of adverse LV changes, LVs showed no changes ($P > 0.284$) in NLRP3 inflammasome activation with exercise. Despite the absence of NLRP3 inflammasome activation after 6 weeks of exercise, it is conceivable that activation may contribute to the TNF-dependent atrial changes induced by acute exercise[33] and TNF-dependent, stretch-mediated signalling cascades.[7,27] However, we were unable to clearly establish either NLRP3 inflammasome activation or its inhibition with atrial *Tnf* gene ablation ($P > 0.270$) following acute exercise in either atria or ventricles, despite trends for increases in both chambers in wild-type (*Cre−*) swim mice (see Supplementary material online, *Figure S12*); uncropped blots are shown in Supplementary material online, *Figure S13*. Furthermore, atrial transcriptome bioinformatics analyses showed no enrichment of NLRP3 inflammasome pathways or genes (*Nlrp3*, *Pycard*, *Casp1*, *Il1b*, *Il18*) following either 2 days or 2 weeks of swim exercise (see Supplementary material online, *Figure S14*). These conclusions were further supported using qtPCR measurements that failed to uncover changes in pro-inflammatory

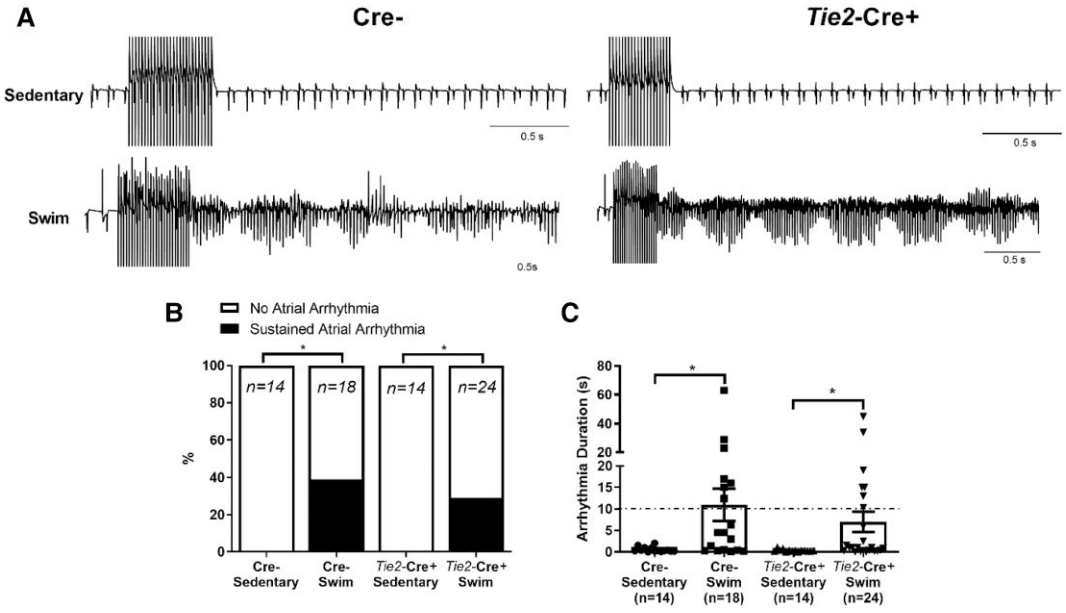

Figure 4 Endothelial-specific *Tnf* ablation does not protect against atrial arrhythmia inducibility in swim-trained mice. Atrial arrhythmia inducibility was determined using intracardiac octopolar catheters inserted into the right atria via the superior jugular vein. (*A*) Representative electrical recordings during and following programmed electrical stimulations in sedentary ($n = 14$ per group) and swim-exercised ($n = 18$ and 24, respectively, per group) mice with (*Tie2-Cre+*) and without (*Cre−*) endothelial cell-specific *Tnf* ablation. Prolonged highly disorganized electrical patterns lasting greater than 10 s, indicative of atrial arrhythmias, were seen in swim-exercised *Tie2-Cre+* and *Cre−* mice. (*B* and *C*) Endothelial cell-specific *Tnf* ablation did not decrease (*P* value from 2 × 2 contingency table using Fisher's exact test) the incidence atrial arrhythmias lasting >10 s or decrease the duration of arrhythmia episodes. Data presented as mean ± S.E.M. *n* values listed within each individual panel. *P* values for arrhythmia durations from Mann–Whitney *U* test with Dunn's multiple comparisons test. $*P < 0.05$; $**P < 0.01$.

(*Tnf*, *Il1b*, *Il6*) genes (see Supplementary material online, *Figure S15*), in the atria or ventricles, independently of *Tnf* gene ablation in atrial cardiomyocytes.

The absence of elevated atrial inflammatory markers or signalling cascades with acute or chronic exercise led us to assess changes in TNF levels with exercise. Despite clear TNF-dependence of adverse atrial changes with exercise, TNF was not elevated 24 h after acute exercise in serum (*Table 2*), or tissue homogenates from atria or ventricles (*Table 2*) for mice with or without atrial-specific *Tnf* gene ablation. These results are consistent with previous exercise studies[34] and suggest that TNF plays a permissive (rather than primary) role in exercise-mediated atrial remodelling, as discussed further below.

4. Discussion

We previously established that blockade of TNF signalling (with either whole-body *Tnf* gene ablation or pharmacological treatment) prevented adverse atrial remodelling and atrial arrhythmia vulnerability induced by intense endurance exercise.[7,15] Given that TNF is produced by multiple cell types in the heart, we sought to determine the cellular origins of TNF underlying the effects of exercise training. We focused our studies on atrial cardiomyocytes and endothelial cells because we previously identified distinct roles of cardiomyocytes and endothelial cells in a TNF-dependent cytokine hierarchy mediating pathological cardiac remodelling in a mouse model of Noonan syndrome, and because both can act as sources of TNF.[25] Our results demonstrate that cell-specific elimination of TNF leads to distinct and non-redundant modulation of atrial responses, but not ventricles, to exercise training. *Tnf* ablation in atrial myocardium protects completely against exercise-induced conduction slowing, hypertrophy, fibrosis, and macrophage infiltration as well as increased arrhythmia inducibility in the atria. In contrast, TNF disruption in endothelial cells only prevented atrial hypertrophy without mitigating the increased fibrosis and vulnerability to atrial arrhythmias induced by exercise training. Importantly, *Tnf* excision in either cell type had no effect on physiological adaptations of autonomic nerve activity, HR responses, and ventricular tissue properties.

Since fibrosis, slowed conduction and hypertrophy are considered trademark features of atria in AF patients that collectively conspire to promote re-entrant arrhythmias,[8] it is reasonable to conclude that these TNF-dependent changes in atrial tissue properties contribute to the increased AF vulnerability seen in exercise-trained mice. Whether, and how, similar atrial changes contribute to AF in endurance athletes is uncertain. In this regard, the atria of elite endurance athletes can display profound atrial enlargement and hypertrophy[35] that far exceeds the hypertrophy seen in ventricles, mirroring that seen in our exercise-trained mice. On the other hand, the presence of atrial fibrosis in elite athletes is hotly debated.[6] Our observation that specific *Tnf* ablation in endothelial cells blocks exercise-induced atrial hypertrophy without preventing either AF inducibility, macrophage infiltration, or atrial fibrosis supports the conclusion that atrial fibrosis plays a more dominant role than hypertrophy in promoting AF vulnerability induced by exercise training. This conclusion is consistent with the generally prominent role of fibrosis in persistent AF patients[36] as well as the observation that the degree of atrial fibrosis varies inversely with conduction velocity, a major determinant of electrical re-entry.[37] However, the incidence of AF inducibility in the exercised mice was reduced by ~24%, and the durations of AF events were ~14% shorter when atrial hypertrophy was attenuated by *Tnf* excision in endothelial cells. Taken together, our findings demonstrate distinct cell autonomous actions of TNF that uncovered differences in the impact of hypertrophy and fibrosis to exercise-induced atrial remodelling and AF vulnerability, which may have implications for mechanisms of AF in elite athletes.

Another potentially important factor contributing to AF in endurance sport is elevated cardiac PNA (vagal tone),[5] which can directly reduce atrial refractoriness via the activation of $I_{K,Ach}$, possibly via RGS down-

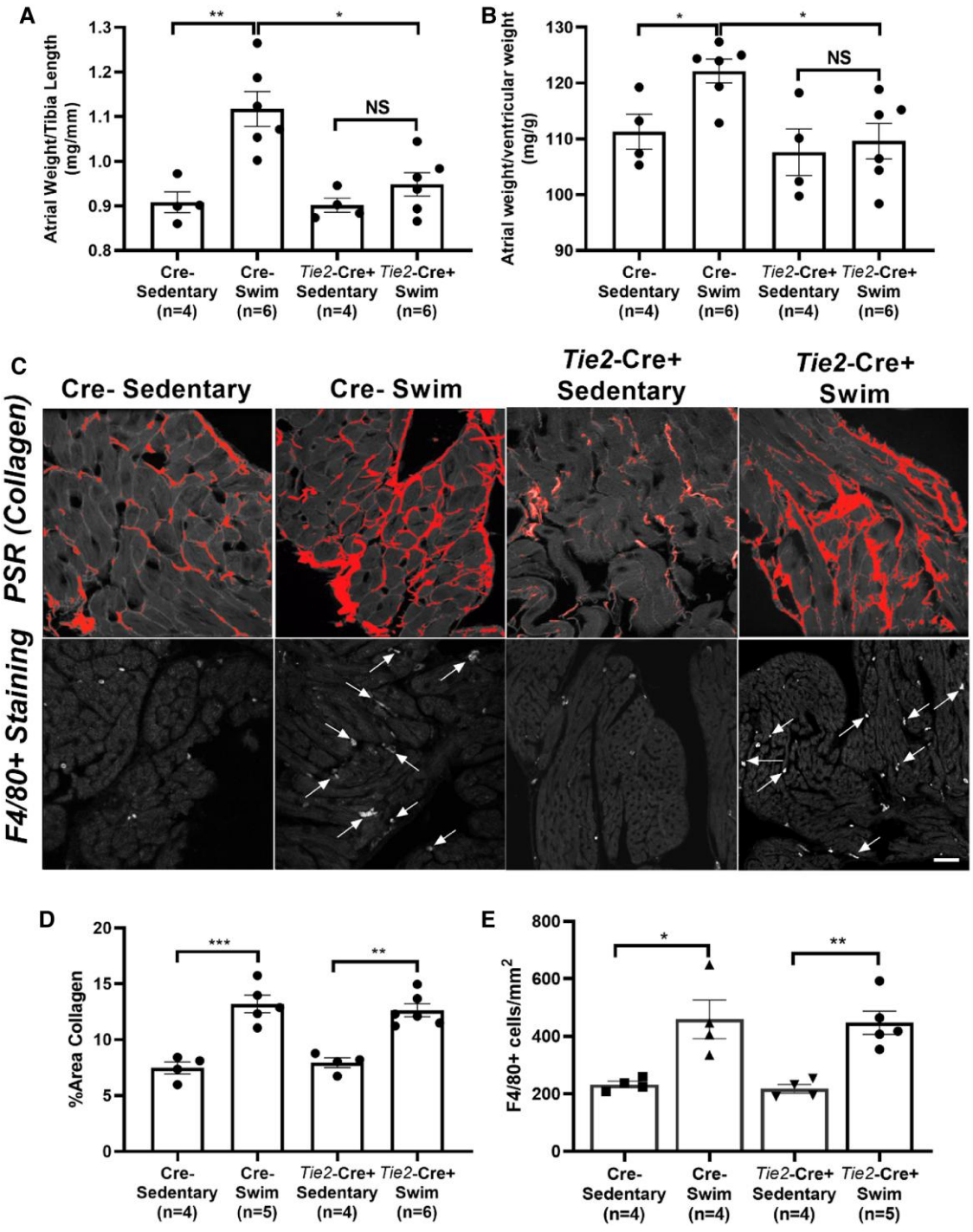

Figure 5 Endothelial cell-specific *Tnf* gene ablation reduces exercise-induced increases in atrial hypertrophy. (*A* and *B*) Atrial weights-to-tibial length and -ventricular weights were increased in swim-trained vs. sedentary mice without endothelial cell-specific *Tnf* excision (*Cre*−). Endothelial-specific *Tnf* ablation attenuated exercise-induced atrial hypertrophy. (*C*) Top panel: Typical confocal micrographs of atrial sections stained with Picrosirius red (PSR). Collagen deposition was increased in swim-trained *Tie2-Cre*+ and *Cre*− mice compared to their sedentary controls. Bottom panel: Confocal micrographs of atrial sections stained with F4/80^{+} to quantify macrophage infiltration (arrows). Macrophage counts were increased in *Tie2-Cre*+ and *Cre*− swim-trained mice compared to their sedentary controls. (*D*) Quantification of collagen deposition (%) shows elevations in atrial fibrosis in *Cre*− ($n = 5$) and *Tie2-Cre*+ ($n = 6$) swim mice compared to their sedentary controls ($n = 4$ and 4, respectively). (*E*) Both *Cre*− ($n = 4$) and *Tie2-Cre*+ ($n = 5$) swim-trained mice showed increased macrophage infiltration (F4/80^{+} cell count) compared to their controls ($n = 4$ and 4, respectively). Data presented as mean ± S.E.M. *P* values from two-way ANOVA with Sidak's multiple comparison tests. *$P < 0.05$; **$P < 0.01$; ***$P < 0.001$. NS, not significant. Scale bar = 50 μm.

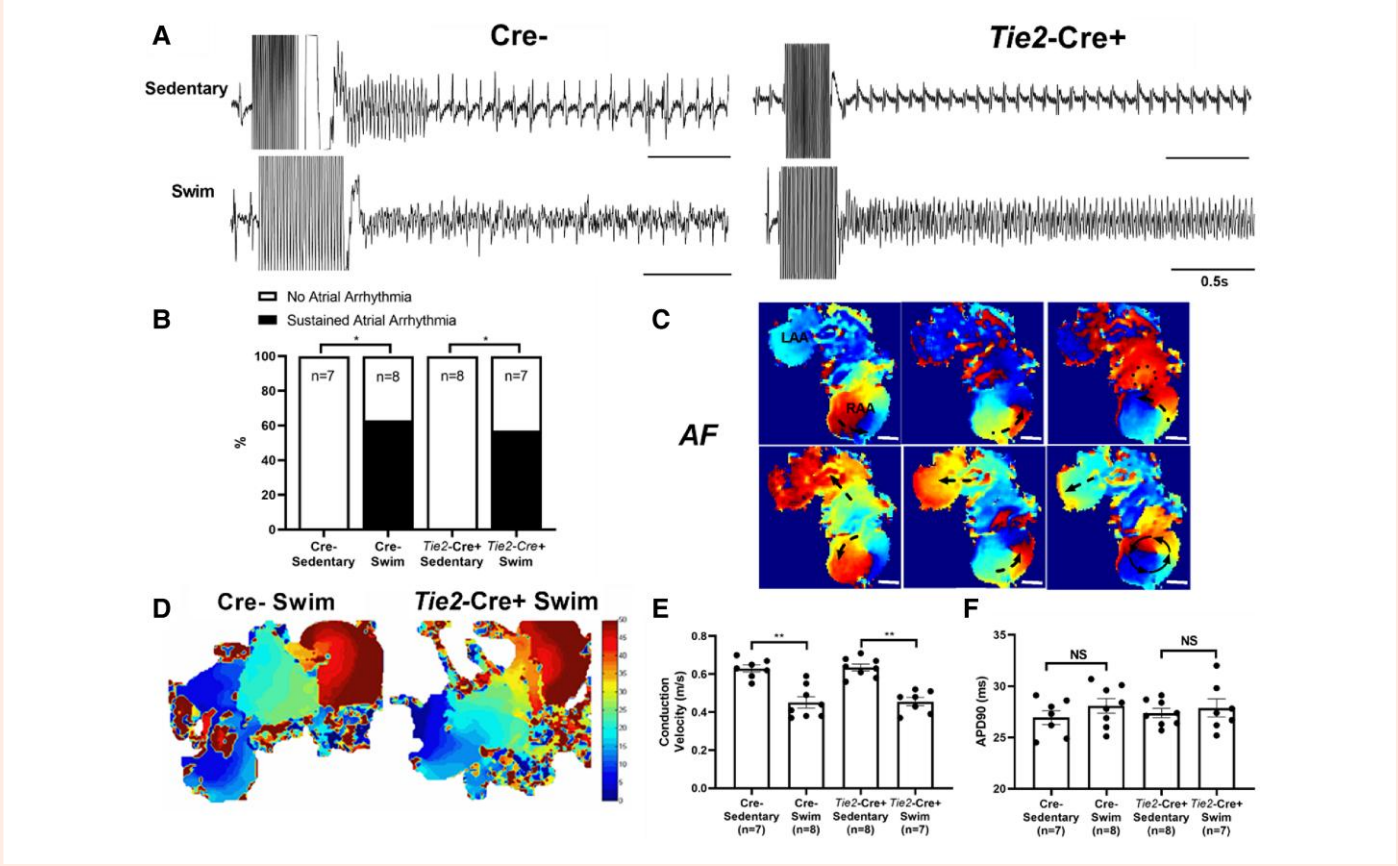

Figure 6 Effects of endothelial-specific *Tnf* ablation on electrical properties on exercise-induced arrhythmias and electrical changes in isolated atria. (*A*) Representative field electrogram recordings from isolated (denervated) atria in *Tie2-Cre*+ and *Cre*− sedentary and exercised mice showing atrial arrhythmia inducibility, with evidence of sustained AF episodes in both *Tie2-Cre*+ and *Cre*− exercised mice only. (*B*) Endothelial-specific *Tnf* ablation (*Tie2-Cre*+) did not protect against sustained (>10 s) atrial arrhythmia inducibility (*P* value from 2 × 2 contingency table with Fisher's exact test) in exercised mice. (*C*) Representative optically-mapped images of AF episodes from rapidly stimulated isolated atria in *Tie2-Cre*+ swim mice. (*D* and *E*) Typical isochrone activation maps and summary results of conduction velocity (CV) measured in right atrial appendages isolated from *Tie2-Cre*+ ($n = 7$) and *Cre*− ($n = 8$) swim-exercised mice revealed that CVs are slowed in *Tie2-Cre*+ and *Cre*− swim mice when compared to their sedentary counterparts ($n = 7$ and 8 per group, respectively). (*F*) In isolated atrial preparations, action potential duration at 90% of repolarization (APD_{90}) were similar between sedentary and exercised mice, in both *Tie2-Cre*+ and *Cre*− groups. The *n* value for individual groups is indicated on bar graphs. Data presented as mean ± S.E.M. *P* values from two-way ANOVA with Sidak's multiple comparison tests. $*P < 0.05$; $**P < 0.01$.

regulation,[28] and which can also promote triggered activity. We found that vagal tone is elevated in intensely exercised mice, and importantly, that this impacts on AF sustainability (i.e. durations of arrhythmic events are reduced by atropine), without affecting the number of mice with inducible AF. These results suggest that structural changes in the atria are the primary factors driving increased AF susceptibility in exercised mice, with vagal tone playing a more modulatory role. In agreement with this conclusion, AF could be readily inducible in isolated (denervated) atria from exercised wild-type mice, even though the APDs in these atria were prolonged compared to sedentary controls. However, it is worth mentioning that increased PNA can modulate inflammatory responses,[38] by dampening and reversing immune-mediated inflammatory responses, which can reduce TNF[39] and AF inducibility[40] in canine models of AF. Indeed, enhanced cardiac vagal tone may limit inflammation induced by exercise, which could explain our inability to measure increased atrial TNF in our model. If such a mechanism contributes to the atrial changes seen with exercise mice, it would appear to involve (or require) atrial cardiomyocyte-, not endothelial-derived TNF since we observed similar degrees of elevation in PNA in all groups of exercised mice while fibrosis was only prevented when TNF is absent in cardiomyocytes. The applicability of these observations to human endurance athletes will require further studies.

We found that the atrial fibrosis and inflammatory cell infiltrates as well as AF vulnerability induced by swim exercise training correlated directly with p38MAPK activation induced by acute bouts of exercise. Specifically, when *Tnf* was excised in atrial cardiomyocytes but not in endothelial cells, acute exercise was unable to activate p38, a stretch- and TNF-dependent MAPK.[31] We believe that these observations are highly relevant to AF pathogenesis because elevated filling pressures and the associated atrial stretch[14] are seen in virtually all conditions that promote AF.[9] Elevated venous filling pressures are also seen during exercise in humans[11] as well as during swimming in mice (reaching 20–40 mmHg),[10] and we show that these elevations were unaffected by *Tnf* excision. Since cardiomyocytes are known to produce large amounts of TNF in response to mechanical stress,[41] which can in turn activate many downstream signalling pathways including canonical NFκB p38,[31] our findings suggest that myocardial-derived TNF may act as a critical mechanosensor that drives atrial changes in response to stretch. In this regard, we previously established that exercise-induced adverse atrial remodelling requires soluble TNF,[15] which is liberated primarily by TACE enzymes. Alternatively, it is possible that our findings reflect repetitive hits of atrial damage with intense exercise rather than stretch. However, we believe that this is unlikely, especially since we previously showed that neither mast cells nor

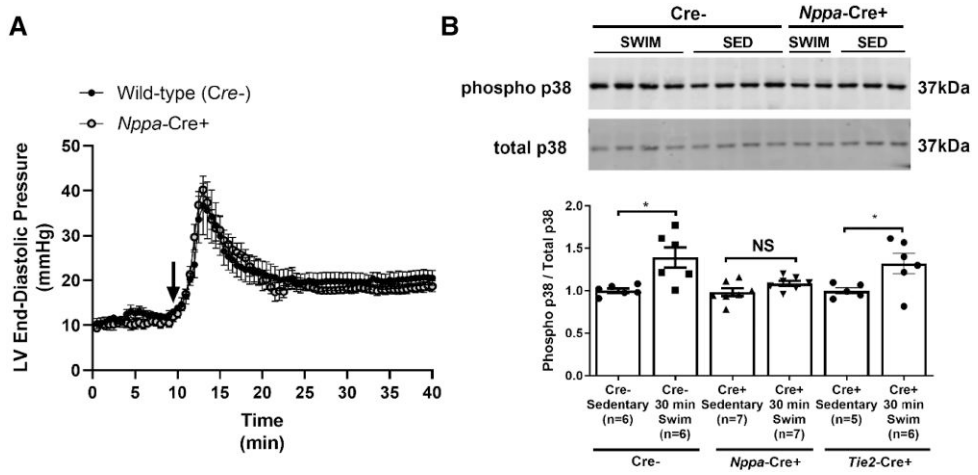

Figure 7 Atrial-specific *Tnf* gene ablation blunts downstream TNF-mediated signal transduction but not mechanical stress with swim exercise. (*A*) Evidence of profound and sustained swim-induced elevations in left ventricular end-diastolic pressures (LVEDPs), an index of left atrial pressures and a stimulus for mechanical stretch, derived from telemetric haemodynamic recordings. No differences in acute (30 min) exercise-induced LVEDPs were observed between *Nppa-Cre+* and *Cre−* mice. Exercise commenced at time = 10 min, as indicated by the black arrow. (*B*) Western blotting analysis revealed increased p38 phosphorylation in the atria (compared to total p38) following 30 min of swim exercise in *Cre−* mice ($n = 6$ per group) compared to sedentary (non-swim) mice. Increases in p38 phosphorylation in response to acute swim were blunted in *Nppa-Cre+* mice ($n = 7$ per group), but not *Tie2-Cre+* mice ($n = 6$). Data are normalized relative to *Cre−* sedentary mice and presented as mean ± S.E.M. Full western blots can be found in the Supplementary material online, Supplementary Materials. *P* values from repeated measures or non-repeated measures two-way ANOVA with Sidak's multiple comparison tests. $^*P < 0.05$. NS, not significant.

neutrophils are elevated with acute and chronic swim exercise,[7] as might occur with myocyte damage. Collectively, our findings support a mechanism in which TNF released from atrial cardiomyocytes sits atop a stretch-dependent cytokine hierarchy that impacts on cardiomyocyte hypertrophy, inflammatory macrophage activation, and fibrosis.

The role of TNF on atrial hypertrophy induced by exercise aligns with our previous studies showing that endothelial cells drive cardiomyocyte hypertrophy in Noonan Syndrome[25] via TNF/IL-6 cytokine hierarchy. Since atrial myocyte-specific *Tnf* ablation also attenuated atrial hypertrophy, it appears that combinatorial interactions and crosstalk between multiple cell types is required for TNF-dependent hypertrophy. In this regard, atrial cardiomyocyte-specific TNF was required for the atrial fibrosis and macrophage infiltration induced by 6 weeks of exercise training that may conceivably involve crosstalk with macrophages that are also stretch-sensitive cells and a major source of TNF.[42] This potential interaction might be of broad interest and important since elevated immune cells are invariably seen in the atria of AF patients[43] thereby providing a mechanistic link between atrial stretch, local inflammation, and AF pathogenesis. These observations align well with studies of cardiac recovery and remodelling in the adult heart.[44] Moreover, endothelial cells are known to express adhesion molecules in a TNF-dependent manner allowing immune cell extravasation into tissues,[45] which supports the possibility that soluble TNF from atrial cardiomyocytes drives endothelial cell-dependent macrophage infiltration in atria. Given the differential effects of cell-specific *Tnf* ablation on exercise-induced atrial remodelling and AF inducibility, it is tempting to speculate that the degree of stretch-activation of TNF in the atria and signal amplification in response to soluble TNF release may determine the tipping point between adaptative and maladaptive remodelling. As atrial hypertrophy is a well-described risk factor for AF vulnerability in endurance athletes,[35] our findings may have important implications on the mechanism of atrial hypertrophy seen in athletes and AF patients. Intriguingly, a recent study identified endocardial TRPC-6 channels as atrial mechanosensors that can serve as load-dependent modulators of endocardial/myocardial interactions.[46]

Although the NLRP3 inflammasome has been implicated recently in AF patients,[47] we did not observe NLRP3 inflammasome activation with chronic intense swim exercise. These observations suggest distinct pathogeneses of exercise-induced AF vs. disease-related AF seen in humans. Consistent with this, we showed previously that chronic endurance exercise did not induce changes in ion channel expression or calcium handling,[7] which are hallmarks of enhanced NLRP3 inflammasome signalling in AF. We did, however, see trends for NLRP3 activation with acute swim exercise in both the atria and ventricles of wild-type mice, but not mice lacking TNF in atrial cardiomyocytes. Further studies will be needed to further explore connections between the NLRP3 inflammasome, TNF, and adverse atrial changes induced by exercise.

As reported previously,[7,15] exercise training affects atria differently from ventricles. We believe that this can be readily explained by differences in chamber compliance (high in atria compared to ventricles) that would directly impact on the degree of chamber stretching in response to elevated diastolic filling pressures that occur during each exercise bout.[7] Consistent with this explanation, atria undergo a ~two-fold greater expansion than ventricles when heart dilations become restricted by pericardium.[7,12] We believe that these observations are relevant because TNF is a mechanosensitive, pro-inflammatory cytokine[16] that is activated by stretch in atrial cardiomyocytes[41] and endothelial cells.[18] Consistent with these observations, serum levels of soluble TNF are elevated[48] along with atrial natriuretic peptide (ANP)[49] (a marker of atrial stretch) in response to mechanical stretch of atrial tissues with exercise. Importantly, we have recently demonstrated chamber-specific transcriptomic remodelling in response to acute (2-day) and chronic (2-week) intense swim training in mice, with hypertrophic and pro-fibrotic signalling pathways disproportionately activated in the atria compared to the ventricles, with TNF playing a permissive (rather than primary) role in atrial, but not ventricular, responses.[27]

4.1 Implications

Although the link between chronic intense endurance exercise and AF prevalence in athletes is well-recognized,[3,6] the basis for this association remains unclear. In this regard, AF in athletes has historically been referred to as 'lone AF' due to the absence of obvious cardiac changes like those seen with CVD.[50] However, animal studies have found that intense endurance

Table 2 Serum and tissue tumour necrosis factor (TNF) levels following 2-day (four-session) acute swim exercise

	Sedentary ($n = 7$)	Swim ($n = 9$)
Serum TNF (pg/mL)	0.81 ± 0.25	1.03 ± 0.16

	Cre− sedentary ($n = 4$)	Cre− swim ($n = 4$)	Nppa-Cre+ sedentary ($n = 4$)	Nppa-Cre+ swim ($n = 4$)
Atrial TNF (pg/mg tissue protein)	3.56 ± 1.65	1.45 ± 0.26	1.80 ± 0.41	2.76 ± 1.05
Left ventricular TNF (pg/mg tissue protein)	2.94 ± 0.74	2.54 ± 0.73	1.10 ± 0.51	1.62 ± 0.27

exercise can induce fibrosis, hypertrophy, and inflammation in the atria, resembling that seen in persistent AF patients.[7,15] The common atrial features of our exercised mice and persistent AF patients raise the possibility that the atria of endurance athletes might also undergo adverse atrial changes, which might explain why endurance athletes, especially veteran athletes, have AF risks rivalling that seen in disease conditions,[4] despite the well-established benefits of regular moderate physical activity on AF risk reduction.[3] Moreover, because AF prevalence is high in conditions associated with elevated filling pressures (i.e. aging, CV disease, and endurance sport exercise),[2] we suggest that elevated venous filling pressures induce atrial changes as a result of tissue stretching that is powerful stimulus for remodelling.[13,14]

Consistent with the TNF requirement in the exercise-induced atrial changes and AF vulnerability, TNF and inflammation[17] have been implicated in AF and its pathogenesis. Moreover, the differential effects of *Tnf* ablation in atrial cardiomyocytes vs. endothelial cells on atrial changes induced by exercise align well with the diverse pleiotropic actions of TNF as well as the many cellular sources of TNF. Indeed, our findings highlight that distinct and non-redundant phenotypes arise not only from immune cells[22] but non-immune cells as well. We speculate that a better understanding of the dynamic cellular interplay in the cytokine hierarchy may provide novel approaches for attenuating and preventing adverse atrial remodelling and AF in AF patients, regardless of their underlying condition.

4.2 Limitations

Although our mouse model provides clear evidence of adverse atrial remodelling and AF promotion with intense exercise, extrapolation of our findings to humans warrants caution. HR increases during exercise is far less in mice (<50%) compared to humans (300–400%), suggesting that increases in stroke volume rather than HR drive increases in cardiac output during exercise in mice. Consequently, atrial stretch may be greater in mice relative to humans during exercise. These differences might explain why adverse atrial remodelling and enhanced AF vulnerability are observed after only 6 weeks of intense exercise in mice. However, swimming is only associated with ~4-4.5 metabolic equivalent tasks (METs)[7] (measured relative to sleeping) in our mice, which is much less than the METs typically associated with 'vigorous' exercise in humans (>6 METs). It should also be emphasized that while our findings support a role for stretch-mediated TNF activation in the exercise-mediated atrial changes, exercise activates a multitude of physiological, metabolic, and biochemical changes in numerous cell types that may or may not require TNF and its associated downstream signalling pathways for influencing atrial responses to exercise.

While we observed clear elevations in macrophage numbers in atria but not ventricles with 6 weeks of exercise that required cardiomyocyte TNF, we did not assess whether these elevations were related to changes in tissue resident macrophages vs. infiltrating monocyte-derived macrophages. Given the complexity of macrophage heterogeneity in tissue homeostasis, tissue damage and repair, future studies characterizing the nature and time course of immune cell responses in exercise and disease models of AF are needed.

Although our studies focused on TNF originating from atrial cardiomyocytes and endothelial cells, TNF from other cell types, such as cardiac fibroblasts,[51] macrophages[42] (discussed above), and other immune cells,[22] may contribute to the complexity of cellular crosstalk mediating adverse atrial remodelling and AF in our model.

Supplementary material

Supplementary material is available at *Cardiovascular Research* online.

Authors' contributions

Experiments were performed at York University Department of Biology. R.L. and P.H.B. were responsible for the conception and design of the work, the acquisition, analysis, and interpretation of data for the work, drafting the work, and revising it critically for important intellectual content. N.P. was responsible for the conception and design of the work, and the acquisition, analysis, and interpretation of data. X.L., S.Y., M.P., R.D., X.G., W.C., C.G., S.Y., F.I., M.W., W.X., and Q.L. were involved in acquisition, analysis, and interpretation of data for the work. S.A.N. generated the $Tnf^{fl/fl}$ mice. V.M.C. generated the mice with atrial cardiomyocyte-specific expression of *Cre*-recombinase. All authors approved the final version of this manuscript and agreed to be accountable for all aspects of the work.

Conflict of interest: None declared.

Funding

Canadian Institutes of Health Research (CIHR) provided a Post-doctoral Fellowship to R.L. P.H.B. acknowledges project grants from the CIHR (MOP-119339, MOP 125950 and PJT-180391), a Canada Research Chair in Cardiovascular Biology from the CIHR, and a John Evans Leader Award for equipment from the Canadian Foundation for Innovation. V.M.C. received support from Fondation Leducq (14CVD01).

Data availability

RNA sequencing data generated in this study can be found in the BioProject database (accession: PRJNA663094). Additional data underlying this article will be shared upon reasonable request to the corresponding authors.

References

1. Krijthe BP, Kunst A, Benjamin EJ, Lip GY, Franco OH, Hofman A, Witteman JC, Stricker BH, Heeringa J. Projections on the number of individuals with atrial fibrillation in the European Union, from 2000 to 2060. *Eur Heart J* 2013;**34**:2746–2751.
2. Lloyd-Jones DM, Wang TJ, Leip EP, Larson MG, Levy D, Vasan RS, D'Agostino RB, Massaro JM, Beiser A, Wolf PA, Benjamin EJ. Lifetime risk for development of atrial fibrillation: the Framingham Heart Study. *Circulation* 2004;**110**:1042–1046.
3. Redpath CJ, Backx PH. Atrial fibrillation and the athletic heart. *Curr Opin Cardiol* 2015;**30**: 17–23.
4. Mont L, Sambola A, Brugada J, Vacca M, Marrugat J, Elosua R, Pare C, Azqueta M, Sanz G. Long-lasting sport practice and lone atrial fibrillation. *Eur Heart J* 2002;**23**:477–482.
5. Prior DL, La Gerche A. The athlete's heart. *Heart* 2012;**98**:947–955.
6. Guasch E, Mont L, Sitges M. Mechanisms of atrial fibrillation in athletes: what we know and what we do not know. *Neth Heart J* 2018;**26**:133–145.
7. Aschar-Sobbi R, Izaddoustdar F, Korogyi AS, Wang Q, Farman GP, Yang F, Yang W, Dorian D, Simpson JA, Tuomi JM, Jones DL, Nanthakumar K, Cox B, Wehrens XH, Dorian P, Backx PH. Increased atrial arrhythmia susceptibility induced by intense endurance exercise in mice requires TNFalpha. *Nat Commun* 2015;**6**:6018.
8. Oakes RS, Badger TJ, Kholmovski EG, Akoum N, Burgon NS, Fish EN, Blauer JJ, Rao SN, DiBella EV, Segerson NM, Daccarett M, Windfelder J, McGann CJ, Parker D, MacLeod RS, Marrouche NF. Detection and quantification of left atrial structural remodeling with delayed-enhancement magnetic resonance imaging in patients with atrial fibrillation. *Circulation* 2009;**119**:1758–1767.
9. Vranka I, Penz P, Dukat A. Atrial conduction delay and its association with left atrial dimension, left atrial pressure and left ventricular diastolic dysfunction in patients at risk of atrial fibrillation. *Exp Clin Cardiol* 2007;**12**:197–201.
10. Lakin R, Debi R, Yang S, Polidovitch N, Goodman JM, Backx PH. Differential negative effects of acute exhaustive swim exercise on the right ventricle is associated with disproportionate hemodynamic loading. *Am J Physiol Heart Circ Physiol* 2021;**320**:H1261–H1275.
11. Reeves JT, Groves BM, Cymerman A, Sutton JR, Wagner PD, Turkevich D, Houston CS. Operation Everest II: cardiac filling pressures during cycle exercise at sea level. *Respir Physiol* 1990;**80**:147–154.
12. Hamilton DR, Dani RS, Semlacher RA, Smith ER, Kieser TM, Tyberg JV. Right atrial and right ventricular transmural pressures in dogs and humans. Effects of the pericardium. *Circulation* 1994;**90**:2492–2500.
13. Burstein B, Nattel S. Atrial fibrosis: mechanisms and clinical relevance in atrial fibrillation. *J Am Coll Cardiol* 2008;**51**:802–809.
14. De Jong AM, Maass AH, Oberdorf-Maass SU, Van Veldhuisen DJ, Van Gilst WH, Van Gelder IC. Mechanisms of atrial structural changes caused by stretch occurring before and during early atrial fibrillation. *Cardiovasc Res* 2011;**89**:754–765.
15. Lakin R, Polidovitch N, Yang S, Guzman C, Gao X, Wauchop M, Burns J, Izaddoustdar F, Backx PH. Inhibition of soluble TNFalpha prevents adverse atrial remodeling and atrial arrhythmia susceptibility induced in mice by endurance exercise. *J Mol Cell Cardiol* 2019; **129**:165–173.
16. Kroetsch JT, Levy AS, Zhang H, Aschar-Sobbi R, Lidington D, Offermanns S, Nedospasov SA, Backx PH, Heximer SP, Bolz SS. Constitutive smooth muscle tumour necrosis factor regulates microvascular myogenic responsiveness and systemic blood pressure. *Nat Commun* 2017;**8**:14805.
17. Ren M, Li X, Hao L, Zhong J. Role of tumor necrosis factor alpha in the pathogenesis of atrial fibrillation: a novel potential therapeutic target? *Ann Med* 2015;**47**:316–324.
18. Charbonier FW, Zamani M, Huang NF. Endothelial cell mechanotransduction in the dynamic vascular environment. *Adv Biosyst* 2019;**3**:e1800252.
19. Hsieh PC, Davis ME, Lisowski LK, Lee RT. Endothelial–cardiomyocyte interactions in cardiac development and repair. *Annu Rev Physiol* 2006;**68**:51–66.
20. Yao C, Veleva T, Scott L Jr, Cao S, Li L, Chen G, Jeyabal P, Pan X, Alsina KM, Abu-Taha ID, Ghezelbash S, Reynolds CL, Shen YH, LeMaire SA, Schmitz W, Müller FU, El-Armouche A, Tony Eissa N, Beeton C, Nattel S, Wehrens XHT, Dobrev D, Li N. Enhanced cardiomyocyte NLRP3 inflammasome signaling promotes atrial fibrillation. *Circulation* 2018;**138**: 2227–2242.
21. Heijman J, Muna AP, Veleva T, Molina CE, Sutanto H, Tekook M, Wang Q, Abu-Taha IH, Gorka M, Kunzel S, El-Armouche A, Reichenspurner H, Kamler M, Nikolaev V, Ravens U, Li N, Nattel S, Wehrens XHT, Dobrev D. Atrial myocyte NLRP3/CaMKII nexus forms a substrate for postoperative atrial fibrillation. *Circ Res* 2020;**127**:1036–1055.
22. Grivennikov SI, Tumanov AV, Liepinsh DJ, Kruglov AA, Marakusha BI, Shakhov AN, Murakami T, Drutskaya LN, Forster I, Clausen BE, Tessarollo L, Ryffel B, Kuprash DV, Nedospasov SA. Distinct and nonredundant in vivo functions of TNF produced by t cells and macrophages/neutrophils: protective and deleterious effects. *Immunity* 2005;**22**:93–104.
23. de Lange FJ, Moorman AF, Christoffels VM. Atrial cardiomyocyte-specific expression of Cre recombinase driven by an Nppa gene fragment. *Genesis* 2003;**37**:1–4.
24. Koni PA, Joshi SK, Temann UA, Olson D, Burkly L, Flavell RA. Conditional vascular cell adhesion molecule 1 deletion in mice: impaired lymphocyte migration to bone marrow. *J Exp Med* 2001;**193**:741–754.
25. Yin JC, Platt MJ, Tian X, Wu X, Backx PH, Simpson JA, Araki T, Neel BG. Cellular interplay via cytokine hierarchy causes pathological cardiac hypertrophy in RAF1-mutant Noonan syndrome. *Nat Commun* 2017;**8**:15518.
26. Lakin R, Guzman C, Izaddoustdar F, Polidovitch N, Goodman JM, Backx PH. Changes in heart rate and its regulation by the autonomic nervous system do not differ between forced and voluntary exercise in mice. *Front Physiol* 2018;**9**:841.
27. Oh Y, Yang S, Liu X, Jana S, Izaddoustdar F, Gao X, Debi R, Kim DK, Kim KH, Yang P, Kassiri Z, Lakin R, Backx PH. Transcriptomic bioinformatic analyses of atria uncover involvement of pathways related to strain and post-translational modification of collagen in increased atrial fibrillation vulnerability in intensely exercised mice. *Front Physiol* 2020;**11**:605671.
28. Guasch E, Benito B, Qi X, Cifelli C, Naud P, Shi Y, Mighiu A, Tardif JC, Tadevosyan A, Chen Y, Gillis MA, Iwasaki YK, Dobrev D, Mont L, Heximer S, Nattel S. Atrial fibrillation promotion by endurance exercise: demonstration and mechanistic exploration in an animal model. *J Am Coll Cardiol* 2013;**62**:68–77.
29. Everett TH IV, Wilson EE, Verheule S, Guerra JM, Foreman S, Olgin JE. Structural atrial remodeling alters the substrate and spatiotemporal organization of atrial fibrillation: a comparison in canine models of structural and electrical atrial remodeling. *Am J Physiol Heart Circ Physiol* 2006;**291**:H2911–H2923.
30. Moe GK, Abildskov JA. Atrial fibrillation as a self-sustaining arrhythmia independent of focal discharge. *Am Heart J* 1959;**58**:59–70.
31. Tenhunen O, Sarman B, Kerkela R, Szokodi I, Papp L, Toth M, Ruskoaho H. Mitogen-activated protein kinases p38 and ERK 1/2 mediate the wall stress-induced activation of GATA-4 binding in adult heart. *J Biol Chem* 2004;**279**:24852–24860.
32. McGeough MD, Wree A, Inzaugarat ME, Haimovich A, Johnson CD, Peña CA, Goldbach-Mansky R, Broderick L, Feldstein AE, Hoffman HM. TNF regulates transcription of NLRP3 inflammasome components and inflammatory molecules in cryopyrinopathies. *J Clin Invest* 2017;**127**:4488–4497.
33. La Gerche A, Inder WJ, Roberts TJ, Brosnan MJ, Heidbuchel H, Prior DL. Relationship between inflammatory cytokines and indices of cardiac dysfunction following intense endurance exercise. *PLoS One* 2015;**10**:e0130031.
34. Nielsen HG, Oktedalen O, Opstad PK, Lyberg T. Plasma cytokine profiles in long-term strenuous exercise. *J Sports Med (Hindawi Publ Corp)* 2016;**2016**:7186137.
35. D'Ascenzi F, Anselmi F, Focardi M, Mondillo S. Atrial enlargement in the athlete's heart: assessment of atrial function may help distinguish adaptive from pathologic remodeling. *J Am Soc Echocardiogr* 2018;**31**:148–157.
36. Dzeshka MS, Lip GY, Snezhitskiy V, Shantsila E. Cardiac fibrosis in patients with atrial fibrillation: mechanisms and clinical implications. *J Am Coll Cardiol* 2015;**66**:943–959.
37. Shiroshita-Takeshita A, Brundel BJ, Nattel S. Atrial fibrillation: basic mechanisms, remodeling and triggers. *J Interv Card Electrophysiol* 2005;**13**:181–193.
38. Pavlov VA, Tracey KJ. The vagus nerve and the inflammatory reflex–linking immunity and metabolism. *Nat Rev Endocrinol* 2012;**8**:743–754.
39. Zhang SJ, Huang CX, Zhao QY, Zhang SD, Dai ZX, Zhao HY, Qian YS, Zhang YJ, Wang YC, He B, Tang YH, Wang T, Wang X. The role of alpha7nAChR-mediated cholinergic anti-inflammatory pathway in vagal nerve regulated atrial fibrillation. *Int Heart J* 2021;**62**: 607–615.
40. Zhao Q, Zhang S, Zhao H, Zhang S, Dai Z, Qian Y, Zhang Y, Wang X, Tang Y, Huang C. Median nerve stimulation prevents atrial electrical remodelling and inflammation in a canine model with rapid atrial pacing. *Europace* 2018;**20**:712–718.
41. Palmieri EA, Benincasa G, Di Rella F, Casaburi C, Monti MG, De Simone G, Chiariotti L, Palombini L, Bruni CB, Saccà L, Cittadini A. Differential expression of TNF-alpha, IL-6, and IGF-1 by graded mechanical stress in normal rat myocardium. *Am J Physiol Heart Circ Physiol* 2002;**282**:H926–H934.
42. Oishi S, Sasano T, Tateishi Y, Tamura N, Isobe M, Furukawa T. Stretch of atrial myocytes stimulates recruitment of macrophages via ATP released through gap-junction channels. *J Pharmacol Sci* 2012;**120**:296–304.
43. Yamashita T, Sekiguchi A, Iwasaki YK, Date T, Sagara K, Tanabe H, Suma H, Sawada H, Aizawa T. Recruitment of immune cells across atrial endocardium in human atrial fibrillation. *Circ J* 2010;**74**:262–270.
44. Lavine KJ, Epelman S, Uchida K, Weber KJ, Nichols CG, Schilling JD, Ornitz DM, Randolph GJ, Mann DL. Distinct macrophage lineages contribute to disparate patterns of cardiac recovery and remodeling in the neonatal and adult heart. *Proc Natl Acad Sci U S A* 2014;**111**: 16029–16034.
45. Chandrasekharan UM, Siemionow M, Unsal M, Yang L, Poptic E, Bohn J, Ozer K, Zhou Z, Howe PH, Penn M, DiCorleto PE. Tumor necrosis factor alpha (TNF-alpha) receptor-II is required for TNF-alpha-induced leukocyte-endothelial interaction in vivo. *Blood* 2007; **109**:1938–1944.
46. Nikolova-Krstevski V, Wagner S, Yu ZY, Cox CD, Cvetkovska J, Hill AP, Huttner IG, Benson V, Werdich AA, MacRae C, Feneley MP, Friedrich O, Martinac B, Fatkin D. Endocardial TRPC-6 channels act as atrial mechanosensors and load-dependent modulators of endocardial/myocardial cross-talk. *JACC Basic Transl Sci* 2017;**2**:575–590.
47. Dobrev D, Heijman J, Hiram R, Li N, Nattel S. Inflammatory signalling in atrial cardiomyocytes: a novel unifying principle in atrial fibrillation pathophysiology. *Nat Rev Cardiol* 2023; **20**:145–167.

48. Bernecker C, Scherr J, Schinner S, Braun S, Scherbaum WA, Halle M. Evidence for an exercise induced increase of TNF-alpha and IL-6 in marathon runners. *Scand J Med Sci Sports* 2013;**23**:207–214.
49. Ohba H, Takada H, Musha H, Nagashima J, Mori N, Awaya T, Omiya K, Murayama M. Effects of prolonged strenuous exercise on plasma levels of atrial natriuretic peptide and brain natriuretic peptide in healthy men. *Am Heart J* 2001;**141**:751–758.
50. Wyse DG, Van Gelder IC, Ellinor PT, Go AS, Kalman JM, Narayan SM, Nattel S, Schotten U, Rienstra M. Lone atrial fibrillation: does it exist? *J Am Coll Cardiol* 2014;**63**:1715–1723.
51. Yokoyama T, Sekiguchi K, Tanaka T, Tomaru K, Arai M, Suzuki T, Nagai R. Angiotensin II and mechanical stretch induce production of tumor necrosis factor in cardiac fibroblasts. *Am J Physiol* 1999;**276**:H1968–H1976.

Translational perspective

Endurance sport is associated with atrial fibrillation (AF), and mouse models show that intense exercise training promotes atrial hypertrophy, fibrosis, inflammation, and AF vulnerability, which requires the mechanosensitive inflammatory cytokine tumour necrosis factor (TNF). We demonstrate that *Tnf* ablation in atrial cardiomyocytes protects fully against atrial changes induced by exercise, whereas endothelial-specific ablation only prevents atrial hypertrophy. Since atrial filling pressures increase markedly during exercise and most clinical conditions linked to AF (hypertension, heart failure, valvular/metabolic diseases), we discuss how atrial stretch may mediate cell autonomous effects of TNF and arrhythmogenic tissue changes in the atria.